

**Does the complex Langevin method give unbiased results?**

L. L. Salcedo\*

*Departamento de Física Atómica, Molecular y Nuclear and Instituto Carlos I de Física Teórica y Computacional, Universidad de Granada, E-18071 Granada, Spain*

(Received 14 October 2016; published 8 December 2016)

We investigate whether the stationary solution of the Fokker-Planck equation of the complex Langevin algorithm reproduces the correct expectation values. When the complex Langevin algorithm for an action  $S(x)$  is convergent, it produces an equivalent complex probability distribution  $P(x)$  which ideally would coincide with  $e^{-S(x)}$ . We show that the projected Fokker-Planck equation fulfilled by  $P(x)$  may contain an anomalous term whose form is made explicit. Such a term spoils the relation  $P(x) = e^{-S(x)}$ , introducing a bias in the expectation values. Through the analysis of several periodic and nonperiodic one-dimensional problems, using either exact or numerical solutions of the Fokker-Planck equation on the complex plane, it is shown that the anomaly is present quite generally. In fact, an anomaly is expected whenever the Langevin walker needs only a finite time to go to infinity and come back, and this is the case for typical actions. We conjecture that the anomaly is the rule rather than the exception in the one-dimensional case; however, this could change as the number of variables involved increases.

DOI: [10.1103/PhysRevD.94.114505](https://doi.org/10.1103/PhysRevD.94.114505)**I. INTRODUCTION**

As it is well known, in the functional integral formulation of quantum field theories, the problem is formally transformed into one of classical statistical mechanics where the action plays the role of Hamiltonian in one more spatial dimension. This entails Wick rotating to Euclidean time, where the functional integral has a better mathematical behavior [1]. In many cases, this is sufficient to make the equivalent Boltzmann weight of the integral real and positive, thereby allowing us to apply Monte Carlo techniques in numerical calculations. Unfortunately, even in the Euclidean formulation a positive weight is not always guaranteed and sometimes one has to deal with complex weights. A typical example comes from the introduction of a baryon number chemical potential in lattice QCD [2]. Whether in field theory or in statistical mechanics, real but nonpositive or more generally complex weights are present in some problems. This is the famous sign (or phase) problem. Although the partition function is well defined, a straight application of the Monte Carlo method is not available, and this makes the problem hard to attack numerically [3]. Many ideas have been proposed to treat the sign problem (see, e.g., [4–23]), with success in particular cases, but it is fair to say that no efficient, systematic, and robust approach exists yet to deal with this problem.

A very general and mathematically sound approach exists to deal with complex weights; this is the reweighting technique [24]. Unfortunately, the method suffers from the ubiquitous overlap problem: by using samples from a different weight, importance sampling is violated and the

problem worsens for large systems, precisely where the Monte Carlo approach would be the most efficient (or less inefficient) method. Another more or less general method is the complex Langevin approach of Parisi [4]. Unlike reweighting, this method only applies to continuous degrees of freedom, and moreover the action of the system must admit a holomorphic extension to the complexified version of the real manifold of physical configurations. Nevertheless, analyticity is not a stringent restriction for typical actions. A further recent technique is based on integration on Lefschetz thimbles [25]. We comment on this in Sec. VIII.

The complex Langevin approach shares an important property with reweighting, namely, it does not spoil the locality properties of the system to be simulated. By locality of an action  $S(x)$  [ $x = (x^1, \dots, x^n)$  is the configuration] we mean that for any variable  $x^i$ ,  $S(x)$  can be written as  $S_1(x) + S_2(x)$  where  $S_1$  does not depend on  $x^i$  and  $S_2$  depends on  $x^i$  and a small number of other variables (the so-called neighbors of  $x^i$ ). This requirement is often crucial for an efficient implementation of a Monte Carlo algorithm. The complex Langevin algorithm is indeed a very intuitive and handy approach, which, from the beginning, attracted much attention [26–31]. Regrettably, unlike the real Langevin method, its complex version has no sound mathematical foundation, and many examples have been found where the method does not converge or converges to a wrong equilibrium solution [7,32–37].

In a typical application with a complex action  $S(x)$ , one needs to compute expectation values of the complex distribution  $P(x) = e^{-S(x)}$  defined on the manifold of configurations of the physical system. In the complex Langevin algorithm, walkers move on the complexified

\*salcedo@ugr.es

manifold producing some normalized probability density  $\rho(z, t)$  there. The whole point of the approach is that after equilibrium has been reached, the stationary density  $\rho(z)$  should reproduce the correct expectation values of  $P(x)$ , in the sense of an analytical extension of the observables. That is,

$$\langle A(x) \rangle_P = \langle A(z) \rangle_\rho, \quad (1.1)$$

where  $A(z)$  refers to holomorphic extension of the observable  $A(x)$ , and  $\langle A \rangle_P$  and  $\langle A \rangle_\rho$  stand for the expectation values on the real manifold with  $P$  and on the complexified manifold with  $\rho$ , respectively.

Following a suggestion in [34], Söderberg first pointed out [38] that other densities  $\rho(z)$  could exist fulfilling the requirement (1.1) not necessarily derived from a complex Langevin approach, and also properties of them were studied there. In [9] such valid densities  $\rho(z)$  defined on the complexified manifold were named *representations* [of the target complex probability  $P(x)$ ]. In that work, properties of the representations were analyzed and explicit constructions were carried out for  $P(x)$  of the form Gaussian times the polynomial of any degree and in any number of dimensions, among others. Necessary and sufficient conditions for the existence of representations were established in [39]. That representations exist quite generally, not only on  $\mathbb{R}^n$  but also on Lie groups, was shown in [40], with some explicit constructions. Representations beyond the complex Langevin have recently been considered in [41,42]. Even more recently, a Gibbs sampling approach to complex probabilities using representations has been described in [23].

There are complex actions for which the complex Langevin algorithm fails to provide a proper representation density  $\rho(z)$ . The above considerations show that this is not an intrinsic problem of those actions, but rather a limitation of the complex Langevin approach. One such example is the one-dimensional action  $S(x) = i\beta_I \cos(x)$  with  $\beta_I$  real and different from zero. The complex Langevin arrives in this case to a  $\rho(z)$  on the complex plane which is independent of  $x$ , thereby predicting vanishing expectation values for all  $e^{ikx}$  except  $k = 0$ . Such an incorrect result is not due to a pathology of this action. Indeed, as shown in [23], just any periodic one-dimensional action can be represented on the complex plane by a positive probability density of the form

$$\rho(z) = Q_1(x)\delta(y - Y) + Q_2(x)\delta(y + Y), \quad (1.2)$$

where the periodic functions  $Q_{1,2}(x)$  are positive for real  $x$ . By decomposing in Fourier modes it can be easily shown that the condition (1.1) is fulfilled by taking

$$Q_{1,k} = \frac{e^{kY} P_k - e^{-kY} P_{-k}^*}{2 \sinh(2kY)}, \quad Q_{2,k} = -\frac{e^{-kY} P_k - e^{kY} P_{-k}^*}{2 \sinh(2kY)}, \quad k \neq 0. \quad (1.3)$$

Clearly these modes correspond to real functions  $Q_{1,2}(x)$ . Moreover, adding suitable zero modes, such  $Q_{1,2}(x)$  are positive by taking  $Y$  above some critical value which depends on the concrete complex action. The same formulas (1.3) apply to nonperiodic actions too, and can be extended to any number of dimensions. We refer to [23] for explicit constructions.

The construction in Eq. (1.2) is a representation with support on two lines parallel to the real axis, and we have noted that positivity of  $\rho$  requires the separation  $2Y$  to be larger than some critical value dependent on  $P(x)$ . This result is quite general: as a rule, the more complex a target complex probability  $P(x)$  is, the more spread on the complex plane should any representation of it be. For instance, if a *real* observable develops a complex expectation value (due to the complex action), such an expectation value will not be reproduced by a density  $\rho(z)$  lying too close to the real axis (where the observable is real). This observation can be made more precise: For any observable  $A(x)$ , let  $\mathbf{A}$  be the set of points  $z$  in the complexified manifold such that  $|A(z)| \geq |\langle A \rangle_P|$ . Then clearly the support of any valid representation  $\rho$  of  $P$  should have some overlap with  $\mathbf{A}$ , since otherwise  $|\langle A \rangle_\rho| < |\langle A \rangle_P|$ .

The overlap condition just mentioned can be applied immediately to the the complex Langevin discussion, through an example noted in [23]. Consider the one-dimensional action  $S(x) = (\beta/4)x^4 + iqx$ , with positive  $\beta$  and  $q$ . In one applies a standard complex Langevin approach here, the walkers will be subject to the usual horizontal diffusion plus a drift with horizontal and vertical components. However, on the real axis the vertical drift is purely downwards, because the term with  $\beta$  does not contribute there. This implies that at equilibrium all the walkers will end up in the lower half plane, since once they move there they have no way to cross the real axis again. It follows that the support of the equilibrium complex Langevin process  $\rho_{\text{CL}}(z)$  is entirely contained in  $\{y \leq 0\}$ . On the other hand, for  $k > 0$ ,  $|e^{-ikz}| = e^{ky} \leq 1$  if  $y \leq 0$ , therefore  $|\langle e^{-ikz} \rangle_{\text{CL}}| \leq 1$ . Yet for  $\beta = 1/2$ ,  $q = 2$ ,  $\langle e^{-ix} \rangle = -4.98$ . So we can conclude that, for this action, the complex Langevin algorithm is necessarily converging to the wrong equilibrium distribution.

It is also known that the Langevin algorithm is afflicted by the segregation problem [43], so it cannot be used to represent a real but nonpositive weight such as  $P(x) = 1 + 2 \cos(x)$ . We emphasize that there is nothing intrinsically wrong with this  $P(x)$  or with the  $(\beta/4)x^4 + iqx$  action above. The two cases can be represented using, for instance, the two-branch approach of Eq. (1.2).

The complex Langevin method has captivated many a researcher due to its elegance [44,45]. Even some tentative proofs of its validity were advanced (see, e.g., [46,47]). Besides, the method has achieved some empirical success in concrete problems [18,48]. Nevertheless, beautiful does not imply correct and after 30 years the mathematical basis

of the method has not been established beyond the rather trivial cases of quadratic actions or real actions. Convergence requires the real part of the eigenvalues of the Fokker-Planck Hamiltonian on the complexified manifold to be non-negative. This property, which is easily established in the real case, has only been observed numerically for certain actions in the complex version [49]. Occasionally, convergence to a correct representation has been guessed from the flow of walkers on the complexified manifold and the nature of the fixed points [50], but this is not conclusive.

Most studies on the validity of the complex Langevin method are based on a mixture of analytical arguments and Monte Carlo simulations analyzing the convergence of the algorithm to correct solutions or not (see, e.g., [32,51–53]). The present work complements those studies. Instead of the Langevin process, our focus is on the Fokker-Planck equation, a second order differential equation on the complexified manifold describing the evolution of  $\rho(z, t)$ , and on its stationary solution,  $\rho(z)$ . While a complex probability admits many different representations, a density  $\rho(z)$  projects to a unique complex probability  $P(x)$ . A natural way to justify the validity of the complex Langevin method is to start with the Fokker-Planck equation fulfilled by  $\rho(z)$ , and to try to show that its projection  $P(x)$  fulfills the projected Fokker-Planck equation (a differential equation on the real manifold) with the target complex probability  $e^{-S(x)}$  as a unique solution. This is the path followed in [7]. However, it was shown there that the projected Fokker-Planck equation may admit further solutions besides  $e^{-S(x)}$ . Moreover, the actual stochastic process may choose one of the wrong solutions. Nevertheless, the cases analyzed in that reference were somewhat artificial, and such spurious solutions are not often found in practice. Here we question the premise, namely, whether or not the naive projected Fokker-Planck equation is actually obtained after projection from the complex to the real manifold. We find that, in general, besides the standard naive terms, additional surface terms may appear in the projected equation, and such anomalous terms introduce a bias in the expectation value of the observables. The crucial role played by boundary terms from integration by parts has been noted before [51]. Here we isolate the anomaly and show in concrete examples that it is nonvanishing. Further, we check, by numerical solution of the stationary Fokker-Planck equation, that the various anomalous relations derived are fulfilled at a numerical level. The origin of the anomaly is the slow falloff at infinity of  $\rho(z)$  in the imaginary direction. In order to analyze the relevant region  $y = \infty$ , we introduce changes of variables which effectively compactify the complexified manifold. The numerical solutions are obtained by solving the differential equation in the original and in the compactified coordinates and matching both solutions. The analysis shows that the presence of an anomaly, and hence a

bias, can be a quite general phenomenon in the complex Langevin approach.

The paper is organized as follows: Spurious solutions are discussed in Sec. II. The form of the anomaly is isolated in Sec. III. In Sec. IV anomalous relations are derived for a periodic action in one dimension. In Sec. V we prove that the anomaly is not vanishing for that action. Generalizations to other periodic actions are discussed in Sec. VI. A nonperiodic action is analyzed in Sec. VII. Finally, conclusions are presented in Sec. VIII.

## II. SPURIOUS SOLUTIONS OF THE COMPLEX LANGEVIN EQUATION

The complex Langevin approach is by far the most frequently used method to construct representations of complex probabilities. The method is easy to implement efficiently and most importantly, if the action  $S(z)$  in  $P = e^{-S}$  is local, i.e., only neighboring sites are coupled, so is the complex Langevin algorithm. The main drawback is that, unlike the real Langevin or other Monte Carlo approaches for positive probabilities, the complex algorithm does not have a sound mathematical basis. In fact, for otherwise regular complex probabilities on the real axis, the complex Langevin process may drift to infinity, or stabilize at a wrong solution. The fact that this cannot be prevented is a serious shortcoming of the method as a reliable tool. Another limitation of principle is that the method requires the target probability  $P(x)$  to have an analytical extension on the complex plane. In practice this is not a crucial problem since in many cases of interest in physics,  $S(z)$  is holomorphic and so is  $P(z)$ .

As we will discuss in a moment, the complex Langevin stochastic process dictates the evolution of a probability density  $\rho(z, t)$  on the complex plane  $\mathbb{C}^n$  representing some complex probability  $P(x, t)$  on the real manifold  $\mathbb{R}^n$ . (Here we are simplifying; the construction can be carried out on more general manifolds, such as Lie groups or coset spaces.) The first problem is whether the stochastic process converges at all. Assuming that this is the case, the main goal is to make sure that complex probability at equilibrium,  $P(x)$ , fulfills the Fokker-Planck-like equation

$$0 = \nabla^2 P(x) + \nabla(\nabla S(x)P(x)). \quad (2.1)$$

Whether this is the case or not will be the subject of the subsequent discussion. Momentarily we assume that Eq. (2.1) holds. One can see that  $P(x) = e^{-S(x)}$  is a solution of the equation and often this is actually the unique solution in the space of normalizable functions. When the solution is unique it automatically follows that the complex Langevin algorithm correctly produces a representation of the target complex probability,  $e^{-S(x)}$ . However, a caveat sometimes overlooked [47] is that one has to seek solutions in the space of distributions, and not only in the space of regular functions: because a distributional  $P(x)$  can be represented

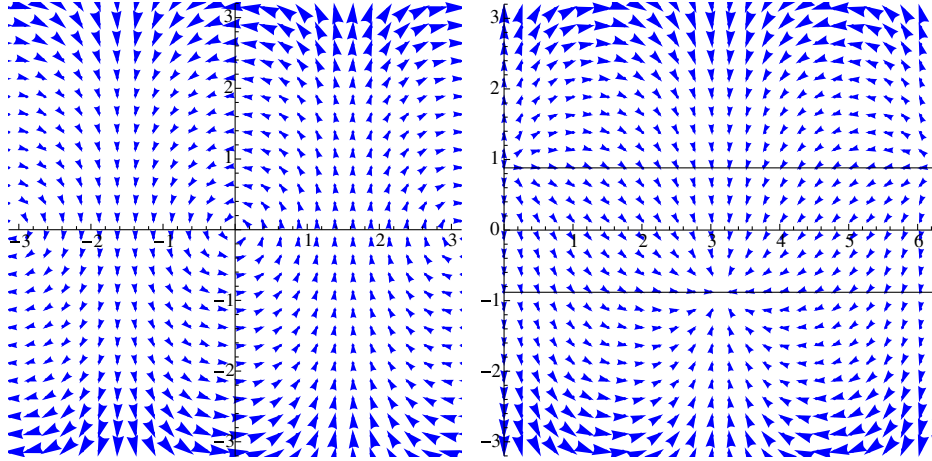


FIG. 1. Velocity fields. Left:  $S = i \cos(z)$  with  $z \in [-\pi, \pi] \times [-\pi, \pi]$ . Right:  $S = \cos(z) + iz$  with  $z \in [0, 2\pi] \times [-\pi, \pi]$ . The two horizontal lines at  $y = \pm \operatorname{arcsinh}(1)$  indicate the strip where  $v_y(z) \leq 0$  for all  $x$ .

on the complex plane, the equilibrium solution  $\rho(z)$  of the Langevin process may also correspond to a distributional complex probability on the real manifold. Without going into details, in [7] (see also [33]) it was shown that spurious solutions can be constructed through the following device (here we consider a one-dimensional problem for simplicity). For any observable  $A(x)$  and path  $\Gamma$  on the complex plane, let

$$\langle A \rangle_{\Gamma} = \frac{\int_{\Gamma} dz P(z) A(z)}{\int_{\Gamma} dz P(z)}, \quad (2.2)$$

where  $P(z) = e^{-S(z)}$  is the analytical extension of the target complex probability. This procedure defines a complex probability distribution  $P_{\Gamma}(x)$  through

$$\langle A \rangle_{\Gamma} = \int dx P_{\Gamma}(x) A(x). \quad (2.3)$$

Whenever  $\Gamma$  connects two zeros (finite or infinite) of  $P(z)$ , or encircles a singularity of  $P(z)$  (so that  $\int_{\Gamma} dz P(z)$  is not zero),  $P_{\Gamma}(x)$  turns out to be a solution of Eq. (2.1). Homologous paths define the same distribution. Concrete examples are shown in [7].

In practice, spurious solutions are only generated by the complex Langevin algorithm if a kernel<sup>1</sup> is chosen to select them or if  $P(x)$  has zeros or singularities close to the real axis. In this regard, it should be noted that even if the action is regular in the natural coordinates, terms of the measure can effectively go into the action and introduce singularities there [55].

<sup>1</sup>A kernel [54] is a modification in the algorithm that produces  $0 = -\partial_i(G^{ij}(x)(\partial_j P(x) + \partial_j S(x)P(x)))$ . When  $G_{ij}(x)$  is a flat metric, the modified process is equivalent to one without kernel but in different variables.

The reason for the preference of the algorithm for smooth complex probabilities is related to the diffusion term which tends to erase any wild  $x$  dependence. For instance, for the action  $S(z) = az^4$  with  $\operatorname{Re}(a) > 0$ , integration along the real or along the imaginary axis defines two different complex probabilities, both fulfilling Eq. (2.1). However, the  $\rho(z)$  produced by the complex Langevin algorithm will be smooth in  $x$  and the Fourier modes  $\langle e^{-ikz} \rangle$  will go to zero for large  $k$ . This corresponds to  $P(x) = e^{-ax^4}$ . For the complex probability distribution defined through integration along the imaginary axis,  $\langle e^{kz} \rangle$  will go to zero for large  $k$  but  $\langle e^{-ikz} \rangle$  will not.

### III. ANOMALY IN THE PROJECTED FOKKER-PLANCK EQUATION

Wrong solutions can appear even for healthy looking complex actions if Eq. (2.1) is not fulfilled due to the presence of anomalous terms. This can be illustrated with one exactly solvable case, namely, that with action<sup>2</sup>

$$S(x) = i\beta_I \cos(x), \quad \beta_I \in \mathbb{R}. \quad (3.1)$$

Here  $x$  is a periodic variable and  $e^{-S(x)}$  is normalizable in  $[0, 2\pi]$ . The corresponding velocity flow is shown in the left panel of Fig. 1. For this action, the Fokker-Planck equation on the complex plane [Eq. (3.4) below] can be solved in closed form and gives<sup>3</sup>

<sup>2</sup>Besides a quadratic action and the trivial case  $\rho(z) = e^{-s(x)}\delta(y)$  when  $S(x)$  is real, we are not aware of further exact equilibrium solutions of any complex Langevin dynamics.

<sup>3</sup>In the periodic case we use the normalizations  $\int_0^{2\pi} dx P(x) = \int_0^{2\pi} dx \int_{-\infty}^{\infty} dy \rho(x, y) = 1$ .

$$\rho(x, y) = \frac{1}{4\pi} \frac{1}{\cosh^2(y)}. \quad (3.2)$$

This density is translationally invariant (with respect to  $x$ ) so it corresponds to  $P(x) = 1/(2\pi)$  and certainly is not a representation of  $P(x) = e^{-i\beta_I \cos(x)}$  unless  $\beta_I = 0$ . Note that the expectation values  $\langle e^{\pm iz} \rangle_\rho$  are not ambiguous since they are absolutely convergent, however they vanish, unlike the correct result  $\langle e^{\pm iz} \rangle = iJ_1(\beta_I)/J_0(\beta_I)$ . The correct results are reproduced by using a representation of the two-branch-type [cf. Eq. (1.2)]. The distribution  $P(x) = 1/(2\pi)$  is not a solution of Eq. (2.1), so this is not one of the spurious solutions discussed in the previous section.

To analyze the problem related to violations of Eq. (2.1) we will consider just the one-dimensional case with no kernels. Since in the literature one can find “proofs” that the complex Langevin method must converge to the correct solution and much of what is known relies on numerical experiments, we would like to reach here mathematically solid conclusions at least for a simple but nontrivial case. In the concrete example considered below [Eq. (4.1)], we find that  $\langle e^{-ikx} \rangle$  is correctly reproduced by the complex Langevin method when  $k = -1, 0, 1, 2, 3, \dots$  but wrong values are obtained for  $k = -2, -3, \dots$  For another study of the reliability of the complex Langevin algorithm see [32].

Recall that complex Langevin is a Markovian process with walker  $z(t)$  moving on the complex plane according to the equation

$$dz(t) = v(z(t))dt + \eta(t)\sqrt{2dt}, \quad v(z) \equiv -S'(z). \quad (3.3)$$

We always assume that the action can be holomorphically extended to the complex plane, so  $S(z)$  is an entire function,  $S'(z)$  is its derivative,  $dt$  the infinitesimal fictitious time step, and  $\eta(t)$  is a real random variable independent for each  $t$  with even distribution under  $\eta \rightarrow -\eta$  and normalized such that  $\langle \eta^2 \rangle = 1$ .

The real and positive probability density  $\rho(z, t)$  of finding the walker at  $z$  at time  $t$ , obeys the following Fokker-Planck equation on the complex plane:

$$\begin{aligned} -\partial_t \rho &= h\rho \equiv -\partial_x^2 \rho + \partial(v\rho) + \partial^*(v^* \rho) \\ &= -\partial_x^2 \rho + \nabla \cdot (v\rho). \end{aligned} \quad (3.4)$$

Here

$$\begin{aligned} \partial &= \frac{1}{2}(\partial_x - i\partial_y), & \partial^* &= \frac{1}{2}(\partial_x + i\partial_y), \\ \mathbf{v} &= (v_x, v_y), & v &= v_x + iv_y. \end{aligned} \quad (3.5)$$

In the complex Langevin process, the walker  $z(t)$  follows a drift  $v(z)$  with a random noise  $\eta$  parallel to the real axis. We will assume that the process reaches an equilibrium distribution  $\rho(z)$ , that is,

$$\begin{aligned} \lim_{t \rightarrow +\infty} \rho(z, t) &= \rho(z), & h\rho(z) &= 0, & \rho &\geq 0, \\ \int d^2z \rho &= 1, \end{aligned} \quad (3.6)$$

for arbitrary initial  $\rho(z, t_0)$ .

For the complex Langevin algorithm to work, Eq. (2.1) must be a consequence of  $h\rho = 0$ . To discuss this matter, let us introduce the projector operator that relates a density  $\rho(z)$  with its associated complex probability  $P(x)$  on the real axis. This projector will be denoted  $K$ ,

$$P(x) = (K\rho)(x). \quad (3.7)$$

The form of the operator  $K$  can be obtained from the relation  $\langle A(x) \rangle_P = \langle A(z) \rangle_\rho$ , for any analytic observable  $A$ ,

$$\int dx dy \rho(x, y) A(x + iy) = \int dx \left( \int dy \rho(x - iy, y) \right) A(x), \quad (3.8)$$

therefore,

$$\begin{aligned} (K\rho)(x) &= \int dy \rho(x - iy, y), \\ \rho(x - iy, y) &\equiv e^{-iy\partial_x} \rho(x, y). \end{aligned} \quad (3.9)$$

The projection involves the analytical extension of  $\rho(x, y)$  as a function of  $x$  (we come back to this point below). The relation is more transparent in terms of the Fourier modes. Although many of the considerations extend to the non-compact case, to be concrete we will consider in what follows the case of periodic  $P(x)$ , with period  $2\pi$ :

$$P(x) = \frac{1}{2\pi} \sum_{k \in \mathbb{Z}} P_k e^{ikx}, \quad \rho(x, y) = \frac{1}{2\pi} \sum_{k \in \mathbb{Z}} \rho_k(y) e^{ikx}. \quad (3.10)$$

For the projection

$$P_k = (K\rho)_k = \int_{-\infty}^{+\infty} dy e^{ky} \rho_k(y). \quad (3.11)$$

Let us note that  $P_k = \langle e^{-ikz} \rangle_\rho$ , as defined from integration on the complex plane, is often conditionally convergent. A suitable prescription is to integrate  $x$  first, and this leads to the expression in Eq. (3.11). Of course, a necessary condition for the complex Langevin approach to work at all is to produce finite expectation values. Therefore, we will assume that for the stationary solution the integrals in Eq. (3.11) are convergent for all  $k$ , and in particular

$$\lim_{y \rightarrow \pm\infty} e^{ky} \rho_k(y) = 0. \quad (3.12)$$

If this is combined with the property

$$\rho_k^*(y) = \rho_{-k}(y), \quad (3.13)$$

which follows from  $\rho(z)$  being real, the stronger statement obtains

$$\lim_{y \rightarrow \pm\infty} e^{|ky|} \rho_k(y) = 0. \quad (3.14)$$

Next, it can be easily verified that the projection operator  $K$  fulfills the following algebraic relations:

$$\begin{aligned} K\partial_x &= \partial_x K, & K\partial_y &= i\partial_x K - 2iK\partial^*, \\ K\partial &= \partial_x K - K\partial^*, & Kf(z) &= f(x)K \text{ (for analytic } f(z)), \end{aligned} \quad (3.15)$$

as well as

$$(K\partial^* p)(x) = \frac{i}{2} p(x - iy, y) \Big|_{y=-\infty}^{y=+\infty}. \quad (3.16)$$

[As usual  $f(x)|_a^b$  stands for  $f(b) - f(a)$ .]

These relations can be used to project the Fokker-Planck equation, Eq. (3.4). This gives, on the real axis,

$$-\partial_t P(x, t) = HP - \mathcal{A}, \quad (3.17)$$

with

$$HP \equiv -\partial_x^2 P + \partial_x(vP), \quad \mathcal{A} \equiv 2iK\partial^*(v_y\rho). \quad (3.18)$$

Assuming that the complex Langevin process converges for large  $t$ , and provided that the *anomalous* term  $\mathcal{A}$  vanishes in that limit, the naive projected Fokker-Planck equation is recovered

$$HP = 0. \quad (3.19)$$

This is just Eq. (2.1).

At a *formal* level the anomaly  $\mathcal{A}$  would be expected to vanish quite generally.<sup>4</sup> Indeed, using Eq. (3.16)

$$\mathcal{A}(x) = -(v_y\rho)(x - iy, y) \Big|_{y=-\infty}^{y=+\infty} := \mathcal{A}(x)_+ - \mathcal{A}(x)_-. \quad (3.20)$$

This is a surface term that would vanish for a sufficiently convergent  $v_y\rho$ .

The anomaly can be obtained in closed form for the action  $S = i\beta_I \cos(x)$ , using the known expression of  $\rho(z)$  and Eq. (3.20). This gives

<sup>4</sup>In what follows, by anomaly we mean the anomaly corresponding to the stationary solution of the Fokker-Planck equation.

$$\mathcal{A}(x)_\pm = \pm \frac{i\beta_I}{4\pi} e^{\pm ix},$$

$$\mathcal{A}(x) = \mathcal{A}(x)_+ - \mathcal{A}(x)_- = \frac{i\beta_I}{2\pi} \cos(x). \quad (3.21)$$

The same result follows from using  $P = 1/(2\pi)$  and the anomalous projected Fokker-Planck equation, Eq. (3.17). The relation

$$\mathcal{A}(x)_+ = -\mathcal{A}(-x)_- \quad (3.22)$$

follows from parity symmetry of the action, and hence of  $\rho(z)$ .

A comment is in order related to the analytical extension implied in  $\rho(x - iy, y)$ . Quite independently of the complex Langevin problem, any sufficiently convergent function  $\rho(x, y)$  on the complex plane will produce finite expectation values for a relevant set of holomorphic observables (sufficiently well behaved at infinity) which includes  $e^{-ikx}$ . So we expect that  $\rho(x, y)$  admits a decomposition in Fourier modes with respect to  $x$ , with finite components  $\rho_k(y)$ . The density  $\rho(x, y)$  itself can have a wild nonanalytic dependence (or even have distributional character) with respect to  $x$ , but still we can formally work with  $\rho(x - iy, y)$  through its Fourier modes  $e^{ky}\rho_k(y)$ . If the sum over  $k$  of these components does not converge [and so  $\rho(x - iy, y)$  does not exist as a function] they still define a distribution and this is enough since in practice the projected complex probability  $P(x)$  [Eqs. (3.7) and (3.9)] or the anomaly  $\mathcal{A}(x)$  [Eq. (3.20)] will be needed within integrals over  $x$  weighted with some observable. In the particular case of  $\rho(x, y)$  produced by the complex Langevin algorithm, we conjecture that the dependence on  $x$  will be regular due to the smoothing effect of the diffusion, so  $\rho(x, y)$  could admit an analytical extension in this case, even if this is not required for our analysis. What will be relevant for the vanishing or not of the anomaly is whether  $e^{ky}\rho_k(y)$  goes to zero sufficiently fast for large  $y$ .

Before proceeding we want to make the following observation: the Fokker-Planck equation can also be written as

$$-\partial_t \rho = -\partial^2 \rho + \partial(v\rho) - \partial^*{}^2 \rho + \partial^*(v^* \rho) - 2\partial\partial^* \rho. \quad (3.23)$$

Upon projection to the real plane, the last term is formally zero in the sense that for sufficiently convergent functions,  $K\partial^* \equiv 0$ . If this term is removed one obtains the separable solution  $\rho = |P|^2$  which is real and positive but never normalizable.  $|P(z)|^2$  is formally a representation of  $P(x)$  since  $\int d^2z A(z)P(z)P(z)^* = \int dz A(z)P(z) \int dz^* P(z)^* = \int dz A(z)P(z) = \langle A \rangle_P$ . As noted in [9], the convolution of a representation with a radially symmetric positive function automatically produces a new representation,

so, in principle,  $|P|^2$  could be transformed into a valid representation by applying a convolution.<sup>5</sup> This is actually the role of the last term  $-2\partial\partial^*\rho = -\frac{1}{2}\nabla^2\rho$ , which implements a radially symmetric diffusion. The quadratic form  $-\partial^2 - \partial^{*2}$  is not positive definite as it has a component of diffusion in the  $x$  direction and another of antidiffusion in the  $y$  direction. The term  $-\frac{1}{2}\nabla^2\rho$  just cancels the antidiffusion. (One can add a further term  $-\lambda\nabla^2$ ,  $\lambda \geq 0$  and still have an algorithm formally equivalent to the complex Langevin. The solution will be more dispersed which, in general, is not what one wants.) So the complex Langevin algorithm is essentially equivalent to sampling  $|P|^2$  but introducing some (minimal) diffusion at each step to obtain a normalizable representation. A problem with this approach is that neither  $|P|^2$  nor the radially symmetric diffusion have a preference for the real axis as an integration path, so spurious solutions are not always screened out.

#### IV. ANALYSIS OF A U(1) ACTION

In this section we will analyze the anomaly problem for the following periodic action:

$$S(x) = \beta \cos(x) + imx, \quad \beta, m > 0, \quad m \in \mathbb{Z}. \quad (4.1)$$

This study is of interest because it would seem that the complex Langevin method should work for this action (see, e.g., [50]). The reason to expect this is that the deterministic flow (i.e., the velocity field  $\mathbf{v}$ ) has an *attractive fixed point* at

$$(x = \pi, y = -y_0), \quad y_0 \equiv \operatorname{arcsinh}(m/\beta). \quad (4.2)$$

(See Fig. 1, right panel.) This point is outside the real axis and this is a desirable property to obtain complex expectation values for real observables such as  $\cos(x)$ . Moreover, if one computes the expectation values  $\langle e^{\pm ix} \rangle$  for various  $\beta$  and  $m$  using the complex Langevin they turn out to be numerically correct.

However, there are reasons for concern. For one thing, actions of the type  $\beta \cos(z)$  with complex  $\beta$  behave as  $\frac{1}{2}\beta e^{\pm iz}$  for  $y \rightarrow \mp \infty$ , so the phase of  $\beta$  can be absorbed by a shift in  $x$  and only the modulus matters. This implies that real or imaginary  $\beta$  are qualitatively similar in the region relevant to the anomaly, and we have already seen that for the imaginary case the algorithm gives incorrect results, at least for  $m = 0$ .

<sup>5</sup>For instance, a Gaussian  $e^{-x^2/a}$  convoluted with  $e^{-x^2/b}$  gives  $e^{-x^2/(a+b)}$ ; a negative  $a$  can be compensated with a sufficiently positive  $b$ .

For another, the flow and the complex Langevin process on the complex plane is qualitative similar whether the real parameter  $m$  is an integer number or not. Regardless of this, there will be some  $\rho(z)$  of equilibrium which certainly will be periodic by construction. Therefore, such  $\rho(z)$  cannot represent  $e^{-S(x)}$ , which is not a periodic function for noninteger  $m$ .

To proceed with the analysis of the action in Eq. (4.1) we will exploit the following observation. For an action of the type:

$$S(x) = S_0(x) + imx, \quad S_0(x) \in \mathbb{R}, \quad m > 0, \quad (4.3)$$

it follows immediately that  $v_y(x, 0) = -m < 0$  for all  $x$ . Consequently a walker below the real axis will never cross it again. If an equilibrium solution exists and is unique, this implies that its support will be contained entirely on the lower half plane,  $y \leq 0$ .

Specifically, for  $S = \beta \cos(x) + imx$  one finds that  $v_y < 0$  on the strip  $|y| < y_0$  (Fig. 1, right panel), thus the support of the equilibrium solution will lie in the half-plane  $y \leq -y_0$ .

$$\rho = 0 \quad \text{for } y > -y_0. \quad (4.4)$$

Another useful property of this action, which holds whenever  $S_0(x)$  is an even function, is that the flow, and hence  $\rho(z)$ , is reflection symmetric with respect to the imaginary axis, even if  $P(x) = e^{-S(x)}$  does not have such a symmetry,<sup>6</sup>

$$\rho(x, y) = \rho(-x, y). \quad (4.5)$$

A direct application of Eq. (3.20) gives for the anomaly (noting that the upper limit  $y \rightarrow +\infty$  vanishes in our case)

$$\begin{aligned} \mathcal{A}(x) = & \left( \frac{1}{2} \beta \cos(x) \sinh(2y) + i\beta \sin(x) \sinh^2(y) - m \right) \\ & \times \rho(x - iy, y) \Big|_{y=-\infty}. \end{aligned} \quad (4.6)$$

At this point an argument can be given suggesting that the anomaly does not vanish: In the periodic case  $x$  is a compact variable, so it can be expected that the random noise tends to flatten the  $x$  dependence of  $\rho$ . Thus, in the large  $y$  limit, the variation with  $y$  will be much more important. Neglecting  $\partial_x \rho$  in the Fokker-Planck equation one obtains (using the Cauchy-Riemann equation  $\partial_x v_x = \partial_y v_y$ )

<sup>6</sup>This emergent symmetry is not the signal of a problem, it also appears in the two-branch representations discussed in the Introduction.

$$0 \approx (\partial_x v_x)\rho + \partial_y(v_y\rho) = \frac{1}{v_y}\partial_y(v_y^2\rho), \quad (4.7)$$

and hence the following estimate is obtained:

$$\rho(x, y) \approx \frac{C(x)}{v_y^2(x, y)}. \quad (4.8)$$

[ $C(x)$  is an integration constant, with respect to  $y$ .] Since one expects  $\rho(x - iy, y)$  to behave like  $\rho(x, y)$  for large  $y$  (if the Fourier mode  $k = 0$  is dominant) this implies in our case

$$\rho(x - iy, y) \sim e^{2y} \quad \text{for } y \rightarrow -\infty. \quad (4.9)$$

This asymptotic behavior allows a nonvanishing anomaly in Eq. (4.6).

Incidentally, the ansatz in Eq. (4.8) will actually be exact when  $v_y$  is a separable function of  $x$  and  $y$ . In this case  $C(x)$  can be chosen in such a way that  $\rho$  depends only on  $y$ . However, the additional condition requiring  $v(z)$  to be a holomorphic function leaves as essentially unique solution that already given in Eqs. (3.1) and (3.2).

The annoying analytic extension implied in  $\rho(x - iy, y)$  in Eq. (4.6) can be dealt with by using Fourier modes. Because  $\rho$  is an even real function of  $x$  it follows that

$$\rho_k(y) = \rho_{-k}(y) = \rho_k^*(y) \quad \forall y, \quad k. \quad (4.10)$$

An easy calculation gives for the anomaly (4.6) in terms of Fourier modes

$$\mathcal{A}_k = \left( \frac{1}{2}\beta \sinh(y)(\rho_{k+1} + \rho_{k-1}) - m\rho_k \right) e^{ky} \Big|_{y=-\infty}, \quad (4.11)$$

which can be simplified using Eq. (3.12):

$$\mathcal{A}_k = -\frac{1}{4}\beta e^{(k-1)y}\rho_{k+1} \Big|_{y=-\infty}. \quad (4.12)$$

This result can be sharpened using Eq. (3.14), which results in

$$\mathcal{A}_k = \begin{cases} 0 & k \geq 0 \\ -\frac{1}{4}\beta e^{(k-1)y}\rho_{k+1}(y) \Big|_{y=-\infty} & k < 0. \end{cases} \quad (4.13)$$

The condition that  $\mathcal{A}_k$  should not diverge (necessary if the complex Langevin algorithm should work at all) implies that actually  $\rho_k$  must vanish at least as  $e^{(2+|k|)y}$  for large negative  $y$ , i.e.,

$$\lim_{y \rightarrow -\infty} e^{-(2+|k|)y}\rho_k(y) < \infty. \quad (4.14)$$

This condition is more restrictive than Eq. (3.14).

According to Eq. (4.13), the first possible anomaly comes from  $k = -1$ ,

$$\mathcal{A}_{-1} = -\frac{1}{4}\beta e^{-2y}\rho_0(y) \Big|_{y=-\infty}. \quad (4.15)$$

In order to see the effect of the anomaly on the expectation values  $\langle e^{-ikx} \rangle = P_k$ , let us rewrite the projected Fokker-Planck equation, Eq. (3.17), in terms of Fourier modes

$$-\partial_t P_k = k(k+m)P_k - \frac{1}{2}\beta k(P_{k+1} - P_{k-1}) - \mathcal{A}_k. \quad (4.16)$$

When  $\partial_t P_k = 0$  (equilibrium) and  $\mathcal{A}_k = 0$  (no anomaly), this recurrence relation (removing a global factor  $k$ ) is that of the Bessel functions. Its unique downward solution, constrained by the conditions  $P_k \rightarrow 0$  for  $k \rightarrow +\infty$  and  $P_0 = 1$ , is

$$P_k = \frac{I_{m+k}(-\beta)}{I_m(-\beta)}. \quad (4.17)$$

These are the correct expectation values of  $e^{-ikx}$  for  $S(x) = \beta \cos(x) + imx$ .

We assume that, as a result of the diffusion term in the complex Langevin,  $P_k \rightarrow 0$  for large  $k$ . Noting that the quantities  $\mathcal{A}_k$  vanish for  $k \geq 0$  and using  $P_0 = 1$ , it follows from Eq. (4.16) that the  $P_k$  obtained by complex Langevin will be correct for all  $k \geq -1$ ,

$$\Delta P_k = 0 \quad \text{for } k \geq -1. \quad (4.18)$$

( $\Delta P_k$  is the shift in the complex Langevin estimate compared to the unbiased result.) The first anomalous (i.e., biased) expectation value takes place for  $P_{-2}$ . Equation (4.16) at equilibrium provides the following relation for  $k = -1$ :

$$\Delta P_{-2} = -\frac{2}{\beta}\mathcal{A}_{-1} = \frac{1}{2}e^{-2y}\rho_0(y) \Big|_{y=-\infty}. \quad (4.19)$$

## V. PROOF OF THE PRESENCE OF ANOMALIES

### A. Compactification and numerical solutions

From inspection of the Fokker-Planck equation or the complex Langevin process, it is not easy to decide whether  $\rho_0(y)$  goes to zero faster than  $e^{2y}$  for large negative  $y$  or not, as required in Eq. (4.19). In order to clarify this issue we will make a change of variables, from  $(x, y)$  to  $(X, Y)$ , or  $(R, \varphi)$  in polar form, such that  $\varphi \equiv x$  and  $y = -\infty$  will be the new origin  $R = 0$ ,



$$\begin{aligned} \varphi = x, \quad R &= -\frac{1}{\sinh(y)} \quad (y < 0), \\ X &= R \cos(\varphi), \quad Y = R \sin(\varphi). \end{aligned} \quad (5.1)$$

The coordinates  $(X, Y)$  only cover the lower half complex plane of  $z$ . This is sufficient in our case. The original manifold was a cylinder due to  $x = 0 \equiv 2\pi$ . In the new coordinates we have compactified the lower end of this cylinder,  $y = -\infty$ , to a point,  $R = 0$ , which is now a regular point of the manifold  $(X, Y)$  (namely, its origin). We want to show that  $R = 0$  is also a regular point of the complex Langevin process in the new variables.

Let us denote  $\sigma$  the new density in coordinates  $(X, Y)$

$$\begin{aligned} \int_0^{2\pi} dx \int_{-\infty}^0 dy \rho &= \int_{\mathbb{R}^2} dX dY \sigma, \quad \rho = \chi R^2 \sigma, \\ \chi &\equiv \sqrt{1 + R^2}. \end{aligned} \quad (5.2)$$

We introduce Fourier modes as usual

$$\sigma = \frac{1}{2\pi} \sum_k e^{ik\varphi} \sigma_k(R), \quad \sigma_k = \sigma_{-k} = \frac{1}{\chi R^2} \rho_k. \quad (5.3)$$

The radial coordinate  $R(y)$  is such that  $\rho \approx 4e^{2y}\sigma$  for large and negative  $y$ , thus

$$\frac{1}{8\pi} \rho_0(y) e^{-2y} \Big|_{y=-\infty} = \frac{\sigma_0(0)}{2\pi} = \sigma \Big|_{R=0} \equiv \sigma(0). \quad (5.4)$$

In this way the leading anomaly, Eq. (4.19), becomes

$$\Delta P_{-2} = 4\pi\sigma(0), \quad (5.5)$$

and its value depends on the value of the density  $\sigma(X, Y)$  at the origin.

In the new coordinates, the Fokker-Planck equation takes the form

$$-\partial_t \sigma = -\partial_\varphi^2 \sigma + \partial_X (v_X \chi \sigma) + \partial_Y (v_Y \chi \sigma) \quad (5.6)$$

with

$$v_X = -mX - \beta, \quad v_Y = -mY, \quad \partial_\varphi = X\partial_Y - Y\partial_X. \quad (5.7)$$

The most relevant condition on the choice of  $R(y)$  is that  $R \sim e^y$ . This ensures that  $(v_X, v_Y)$  is finite at  $y \rightarrow -\infty$ . The precise form of  $R(y)$  in Eq. (5.1) is such that  $v_Y$  has no contribution from  $\beta$ . The function  $\chi$  is harmless since it equals 1 at the origin and is everywhere smooth (in fact analytic) on the  $(X, Y)$  plane. For the present discussion  $\chi$  can be absorbed in  $\sigma$ .

The flow  $(v_X, v_Y)$  is displayed in Fig. 2. We can see from Eq. (5.7) that in  $(X, Y)$  coordinates the deterministic part of the flow is just an inwards radial field with the center at the

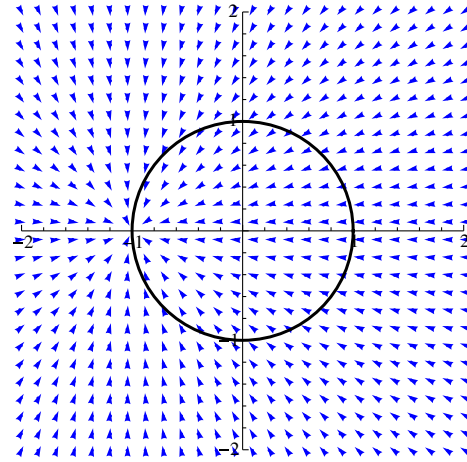


FIG. 2. Velocity field of  $S = \cos(z) + iz$  in variables  $(X, Y)$  in the range  $[-2, 2] \times [-2, 2]$ . The fixed point is at  $(-1, 0)$ . The circle indicates the boundary of the support of the equilibrium solution, i.e., the locus of  $y = -y_0$ . The diffusion moves the walker along circles centered at the origin (not displayed in the figure).

attractive fixed point  $(X = -R_m, Y = 0)$ , with  $R_m \equiv \beta/m$ . The point  $R = 0$  (corresponding to  $y = -\infty$ ) is not special in any way for that flow. On top of this,  $-\partial_\varphi^2 \sigma$  is an angular diffusion term which accounts for random shifts in the angle  $\varphi$  of the walker without changing  $R$ . So this diffusion term does not directly produce an increase nor decrease of the density  $\sigma$  at the origin.

The stochastic angular jumps are of order 1 (times  $\sqrt{dt}$ ) in the variable  $\varphi$  but they are small in the  $(X, Y)$  variables as  $R$  approaches zero. The fields  $(v_X, v_Y)$  and  $\partial_\varphi$  are regular everywhere. In the  $(X, Y)$  variables  $R = 0$  is a regular point of the stochastic process and there is no mechanism at work that would enforce  $\sigma(0) = 0$ . The conclusion is that  $\sigma(0) > 0$  and there is a bias in the complex Langevin method already for  $P_{-2}$ .

The conclusion just mentioned is confirmed by numerical solutions of Eq. (5.6) for the stationary case (see Fig. 3). Among the various numerical approaches used (including polar and Cartesian coordinates), we have obtained the best result by using Fourier modes for the dependence on the angular variable  $\varphi$  (rather than directly a mesh on  $\varphi$ ) and a regular grid for  $R$ . For the solution displayed in Fig. 3 we have used 64 Fourier modes for  $\varphi$  and 64 points in  $R$ . We have carried out calculations for several values of  $\beta$  and  $m$ . As it would be expected, the value of  $\sigma(0)$ , and hence the anomaly, is enhanced for small values of  $\beta$  or large values of  $m$ .

The expectation values  $P_k$  numerically obtained from this  $\sigma(X, Y)$  agree well with the Bessel function exact result for  $k = +1, -1, 2$ . For  $k = -2$ , the exact expectation value is  $P_{-2} = 1$ . Instead of this, numerically one obtains  $P_{-2} = 4.86$  for  $\beta = 0.5$  and  $m = 1$ . This bias is quite consistent with the relation (5.5),

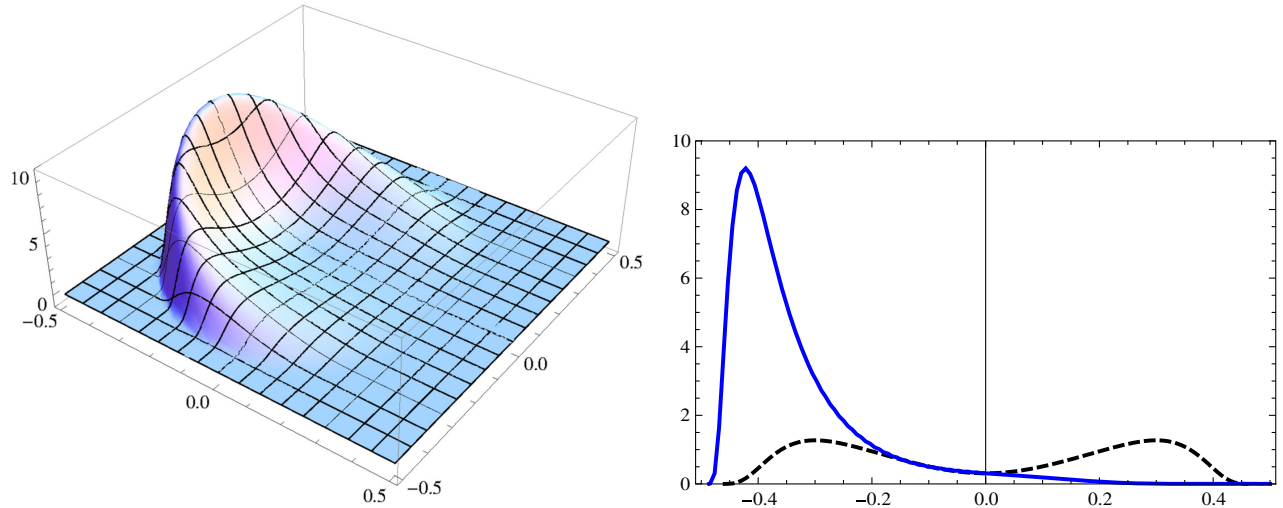


FIG. 3. Function  $\sigma(X, Y)$  for  $\beta = 0.5$  and  $m = 1$ . Left:  $\sigma$  on the  $(X, Y)$  plane. The support is located on  $R \leq R_m = \beta/m$ . The numerical calculation uses 64 Fourier modes in  $\varphi$  and 64 points in the mesh of the variable  $R$ . Numerical derivatives in  $R$  were obtained using 5 points. Right: Sections of  $\sigma(X, Y)$  along the  $X$  (solid blue line) and  $Y$  (dashed black line) axes.  $\sigma(0) = 0.310$ .

$$\Delta P_{-2} = 3.86, \quad 4\pi\sigma(0) = 3.89 \quad (\beta = 0.5, m = 1). \quad (5.8)$$

A standard complex Langevin simulation also correctly reproduces  $P_k$  for  $k = +1, -1, 2$  but becomes noisy for  $k = -2$ .

As we mentioned before, the unphysical case of non-integer  $m$  is qualitatively similar to that of integer  $m$  as regards to the complex Langevin process on the complex plane, and this is also obvious from Eq. (5.7). Remarkably, the arguments leading to Eqs. (4.18) and (4.19) hold for noninteger  $m$  as well and we have confirmed this numerically: For  $m = 0.5$  or  $m = \sqrt{2}$  we still find that the  $P_k$  as obtained from  $\sigma(X, Y)$  reproduce Eq. (4.17) for  $k \geq -1$  whereas  $P_{-2}$  fulfills (5.5) at a numerical level.

## B. Proof of the presence of anomalies from analyticity

Because establishing in an unambiguous manner the existence of a bias in the expectation values of  $e^{-ikx}$  is important, we provide a different argument, based on the analyticity of  $\sigma(X, Y)$ . In the absence of angular diffusion, the walkers would accumulate at the attractive fixed point ( $X = -R_m, Y = 0$ ) and, at equilibrium,  $\sigma$  would become a Dirac delta there. The diffusion moves the walkers along circumferences centered at the origin. The result (see Fig. 3) is an equilibrium distribution with support on the disk  $R \leq R_m$ . The coefficients of the differential equation (5.6) are real-analytic functions at all points, so one should expect that  $\sigma$  is real analytic for  $R < R_m$ . Certainly it cannot be analytic on  $R = R_m$  because  $\sigma$  becomes identically zero for  $R > R_m$  but  $\sigma$  should be  $C^\infty$  there (except at the fixed point) since the vanishing of the function is not imposed as a boundary condition; instead it follows automatically from the differential equation (this is also

observed numerically). The only point where  $\sigma$  may be nonsmooth is at the fixed point. There, the vanishing of  $v_X$  and  $v_Y$  allows us to have a discontinuous radial derivative of  $\sigma$  (although the function itself is continuous). The angular derivative must be continuous due to the smoothing effect of the diffusion. At equilibrium  $\sigma$  fulfills the differential equation at all points except at the fixed point. As a distribution,  $\sigma$  fulfills the differential equation everywhere.

Therefore, the origin is a regular point of  $\sigma(X, Y)$  and this can be used to show that not all the anomalies  $\mathcal{A}_k$  can vanish simultaneously. First note that the nontrivial anomalies, Eq. (4.13), can be expressed as

$$\mathcal{A}_{-k-1} = -\beta \left( \frac{2}{R} \right)^k \sigma_k(R) \Big|_{R=0}, \quad k \geq 0. \quad (5.9)$$

That  $\sigma$ , or equivalently  $\chi\sigma$ , is real analytic at  $R = 0$  implies that

$$\chi\sigma_k = R^{|k|} f_k(R^2), \quad (5.10)$$

where the functions  $f_k(\xi)$  are also analytic. Thus,

$$\mathcal{A}_{-k-1} = -\beta 2^k f_k(0), \quad k \geq 0. \quad (5.11)$$

So, analyticity of  $\sigma$  already guarantees that the anomalies  $\mathcal{A}_k$  are finite (instead of divergent).

Let us assume that all anomalies were vanishing. In this case,  $f_k(0) = 0$  for all  $k$  (recall that  $f_k = f_{-k}$  since  $\sigma_k$  and  $\rho_k$  have the same property). This merely implies that  $\sigma = R^2 \tau$  with  $\tau(X, Y)$  analytic, but it is not inconsistent with  $\sigma$  being analytic. To find a contradiction one must resort to the equilibrium Fokker-Planck equation. In terms of the  $f_k(\xi)$  ( $\xi \equiv R^2$ ) the equation takes the form

$$\begin{aligned}
0 &= -2m(f_0 + \xi f'_0) - 2\beta(f_1 + \xi f'_1), \\
0 &= \left(\frac{k^2}{\chi} - m(k+2)\right)f_k - \beta(k+1)f_{k+1} - 2m\xi f'_k \\
&\quad - \beta(f'_{k-1} + \xi f'_{k+1}) \quad (k \geq 1), \tag{5.12}
\end{aligned}$$

where the prime indicates differentiation with respect to  $\xi$ .

Incidentally, the first equation in (5.12), corresponding to  $k=0$ , is equivalent to the condition that at equilibrium no net flux traverses any  $y = \text{constant}$  line,  $\int dx v_y \rho = 0$ . That equation admits the closed solution  $\sigma_1 = -\frac{m}{\beta} R \sigma_0$ . Since  $|\sigma_k| \leq \sigma_0$  one would obtain a contradiction for  $R > R_m$ . The resolution is that  $\sigma \equiv 0$  for  $R > R_m$ .

Coming back to the proof, let us assume that  $f_k(0) = 0$  for all  $k$  (no anomaly). Setting  $\xi = 0$  in the second equation in (5.12) immediately implies  $f'_k(0) = 0$  for all  $k$  as well. From this, taking a derivative with respect to  $\xi$  and setting  $\xi = 0$  one obtains in turn  $f''_k(0) = 0$ . In fact, by induction, having already  $f_k^{(n)}(0) = 0$  for  $0 \leq n \leq N$ , it follows that  $\partial_\xi^N(\xi f'_k)(0) = 0$ , so applying  $\partial_\xi^N$  to the equation and taking  $\xi = 0$  one concludes  $f_k^{(N+1)}(0) = 0$ . Now, if all the derivatives of the  $f_k(\xi)$  vanish at a point and the functions are analytical they must be identically zero, along with  $\sigma$  for all  $(X, Y)$ . This incorrect conclusion is avoided if some of the anomalies are not zero.

### C. Alternative proof of the presence of anomalies

We have just shown for  $S = \beta \cos(x) + imx$  ( $\beta \in \mathbb{R}$ ) that the analyticity of  $\sigma(X, Y)$  plus the assumption of a vanishing of all anomalies would imply the absurd conclusion  $\sigma(X, Y) \equiv 0$ . Here we want to show that a contradiction can be obtained assuming only that all the Fourier modes  $\rho_k(y)$  fall off exponentially for large negative  $y$ . This is a weaker assumption because analyticity requires positive integer powers of  $e^y$  and here we allow fractional powers.

Specifically we assume

$$\begin{aligned}
\forall k \geq 0 \quad \lim_{y \rightarrow -\infty} e^{-\alpha_k y} \rho_k(y) &= a_k, \\
\lim_{y \rightarrow -\infty} e^{-\alpha_k y} \rho'_k(y) &= a_k \alpha_k, \tag{5.13}
\end{aligned}$$

(the prime indicates derivative with respect to  $y$ ) with

$$\alpha_k = k + 2 + \delta_k, \quad \delta_k \geq 0, \quad a_k \neq 0. \tag{5.14}$$

The condition  $\delta_k \geq 0$  implements Eq. (4.14). The corresponding anomaly vanishes if  $\delta_k > 0$ .

The Fokker-Planck equation in terms of Fourier modes of  $\rho$  takes the form

$$\begin{aligned}
0 &= k^2 \rho_k - m \rho'_k + \frac{\beta}{2} \cosh(y) ((k+1)\rho_{k-1} - (k-1)\rho_{k+1}) \\
&\quad + \frac{\beta}{2} \sinh(y) (\rho'_{k-1} + \rho'_{k+1}). \tag{5.15}
\end{aligned}$$

Using  $\rho_k \sim a_k e^{\alpha_k y}$  and retaining the leading terms yields, for  $k \geq 1$ ,

$$\begin{aligned}
0 &= (k^2 - m(k+2 + \delta_k)) a_k e^{(k+2+\delta_k)y} - \frac{\beta}{4} a_{k-1} \delta_{k-1} e^{(k+\delta_{k-1})y} \\
&\quad - \frac{\beta}{4} (2k+2 + \delta_{k+1}) a_{k+1} e^{(k+2+\delta_{k+1})y} + \text{subleading}. \tag{5.16}
\end{aligned}$$

If we assume that all  $\delta_k > 0$  (no anomalies), it follows that the term with  $a_{k-1}$  does not vanish (because  $\delta_{k-1} \neq 0$ ) and this term will be dominant, thus violating the equation, unless  $\delta_{k-1}$  is sufficiently large to match the two other terms. Specifically,

$$\delta_{k-1} \geq 2 + \min(\delta_k, \delta_{k+1}) \quad \forall k > 0. \tag{5.17}$$

However, it is easy to see that such a strict condition is unattainable. Starting from some large  $N$ , the assumption  $\delta_N, \delta_{N-1} > 0$  implies  $\delta_{N-2} > 2$ ; in turn this implies  $\delta_{N-3} > 2$  and hence  $\delta_{N-4} > 4$ , and eventually  $\delta_{N-2n} > 2n$  whenever  $2n \leq N$ . But  $N$  is arbitrary, thus Eq. (5.17) can only hold if  $\delta_k$  is larger than any even number, i.e.,  $\delta_k = \infty$ . In other words, any exponential falloff is incompatible with the assumption of no anomalies. Since a falloff faster than exponential seems incompatible with the complex Langevin algorithm we conclude that Eq. (2.1) gets an anomaly for the action  $S = \beta \cos(x) + imx$ .

The behavior  $\rho \sim e^{2y}$  not only gives rise to anomalies in Eq. (2.1), it also entails that the integrals  $\int d^2z \rho(z) e^{-ikz}$  are not absolutely convergent for  $|k| \geq 2$ , although they can be given a natural meaning by expressing them in terms of Fourier modes. The conditional convergence implies that the variance would diverge in a straight Monte Carlo approach of those expectation values. Once again we point out that there is nothing pathological with the action  $\beta \cos(x) + im$  itself; any holomorphic observable on the finite complex plane has an absolutely convergent expectation value using a two-branch representation of the type described in the Introduction, since the support of such representations is bounded.

## VI. GENERALIZATION TO OTHER U(1) ACTIONS

### A. Action $\beta \cos(x)$ with complex $\beta$

As for generalizations of the previous analysis to other actions, let

$$S(x) = \beta_1 e^{ix} + \beta_{-1} e^{-ix} + imx, \quad \beta_{\pm 1} \in \mathbb{C}, \quad m \in \mathbb{Z}. \quad (6.1)$$

Following similar steps as for  $S = \beta \cos(x) + imx$  one easily obtains [using Eq. (3.12)]

$$\begin{aligned} \mathcal{A}_k = & -\frac{1}{2} \beta_1^* e^{(k-1)y} \rho_{k+1}(y) \Big|_{y=-\infty} \\ & -\frac{1}{2} \beta_{-1}^* e^{(k+1)y} \rho_{k-1}(y) \Big|_{y=+\infty}. \end{aligned} \quad (6.2)$$

$\mathcal{A}_0$  must vanish since this is equivalent to conserving the number of walkers and we have already assumed that the process has a stable normalizable equilibrium solution. For the remaining anomalies, in the present case there are no symmetries helping to remove some of them. In particular, barring accidental cancellations there will be anomalies  $\mathcal{A}_{\pm 1}$  coming from  $\rho_0(y)$  at  $y = \pm\infty$ . In fact, doing changes of variables  $R \sim e^{\mp y}$  to compactify  $y = \pm\infty$  as before, one finds again that the points at infinity are regular, the density in the transformed coordinates are finite (nonzero) and these anomalies do not vanish. These two anomalies contaminate all the expectation values through the recurrence relation. The action  $S = i\beta_I \cos(x)$  illustrates this effect. There all the  $\mathcal{A}_k$  vanish except  $\mathcal{A}_{\pm 1}$  (due to  $\rho_k = 0$  for  $k \neq 0$ ) and all expectation values other than  $P_0$  are incorrect (they vanish).

In order to sustain the previous arguments more quantitatively, let us consider an action of the type

$$S(x) = \beta \cos(x), \quad \beta \in \mathbb{C}. \quad (6.3)$$

This action is an even function of  $x$ ; correspondingly, the equilibrium solution of the Fokker-Planck equation,  $\rho(z)$ , is an even function of  $z$ .

We have proceeded to numerically solve the Fokker-Planck equation at equilibrium. The differential equation can be written in variable  $z = x + iy$ ; nevertheless, in order to study the region of large  $|y|$ , relevant for anomalies, it is convenient to use additional suitable variables. Specifically, we use the variables  $(X, Y)$  introduced in Eq. (5.1), and the associated density  $\sigma(X, Y)$ . These variables compactify the complex plane and have the virtue that the corresponding drift has a finite velocity at  $X = Y = 0$  with vanishing diffusion there. The variables  $(X, Y)$  only cover the lower half-plane  $y < 0$ ; however, since  $\rho(z)$  is an even function we can work on that lower half-plane without loss of generality.

Our approach has been to solve the differential equation for  $\rho(x, y)$  on the strip  $-y_c < y < y_c$  (actually  $-y_c < y < 0$  suffices due to the symmetry) and solve for  $\sigma(X, Y)$  on the disk  $R < R_c$ , where  $R_c = 1/\sinh(y_c)$ . The two solutions are matched at  $R = R_c$ . The matching parameter  $y_c$  is chosen for a given  $\beta$  attending to numerical convenience. Once again we use Fourier modes for the dependence on

the variable,  $x \equiv \varphi$ , in both sectors, and regular meshes for  $y$  and  $R$ . The correct boundary condition at  $R = 0$  is selected by imposing that no net flux passes through the origin (or in fact any circle  $R = \text{constant}$ , we take  $R = R_c$ ).

The exact solution is known for purely imaginary non-vanishing  $\beta$ , namely,

$$\rho = \frac{1}{4\pi} \frac{1}{\cosh^2(y)}, \quad \sigma = \frac{1}{4\pi} \frac{1}{\chi^3(R)} \quad (\beta = -\beta^*). \quad (6.4)$$

[ $\chi(R) \equiv \sqrt{1 + R^2}$ .] Note that the integral of  $\sigma$  over the  $(X, Y)$  plane is  $1/2$  since this covers only  $y < 0$ .

A numerical solution for  $\beta = 0.25 + i0.5$  is displayed in Fig. 4. The matching of the two sectors has been chosen at  $R_c = 2$ . The two forms  $\rho(x, y)$  (left) and  $\sigma(X, Y)$  (right) are shown. As one would anticipate, for this  $\beta$  the value of  $\rho(0)$  is larger than  $1/(4\pi) \approx 0.08$  while  $\sigma(0) < 1/(4\pi)$ . The value  $1/(4\pi)$  corresponds to purely imaginary  $\beta$  [see Eq. (6.4)]. The presence of a real part in  $\beta$  brings the distribution closer to the real axis, hence, enhancing  $\rho(0)$  and quenching  $\sigma(0)$ . As shown subsequently, Eq. (6.6), a nonzero value of  $\sigma(0)$ , as clearly displayed in Fig. 4 (right panel), implies the presence of an anomaly in the projected Fokker-Planck equation.

Regarding the anomaly for the actions  $\beta \cos(x)$ , since the Fokker-Planck equation preserves the parity of the action, one has

$$\mathcal{A}_k = \mathcal{A}_{-k}. \quad (6.5)$$

From Eq. (6.2) and Eq. (3.14), it follows that

$$\mathcal{A}_1 = -\frac{1}{4} \beta^* e^{2y} \rho_0(y) \Big|_{y=+\infty} = -\beta^* \sigma(0) = -2\pi\beta^* \sigma(0). \quad (6.6)$$

Therefore, as expected there is an anomaly whenever  $\sigma(X, Y)$  is sizable near  $R = 0$ . This is a regular point of the stochastic process in the new variables and  $\sigma(0)$  is nonvanishing in general (Fig. 4).

To see the bias introduced by the anomaly of Eq. (6.6) on the expectation values, we again make use of the projected Fokker-Planck equation, Eq. (4.16), with  $m = 0$  and complex  $\beta$ . Selecting the stationary case,  $\partial_t P_k = 0$ , gives for  $k = 1$ , using  $P_0 = 1$ ,

$$0 = P_1 - \frac{\beta}{2} (P_2 - 1) + 2\pi\beta^* \sigma(0). \quad (6.7)$$

This equation holds with  $\sigma(0) = 0$  for the exact expectation values in Eq. (4.17). Therefore, the biases  $\Delta P_1$ ,  $\Delta P_2$  introduced by the anomaly fulfill the relation

$$\Delta P_1 - \frac{\beta}{2} \Delta P_2 = -2\pi\beta^* \sigma(0). \quad (6.8)$$

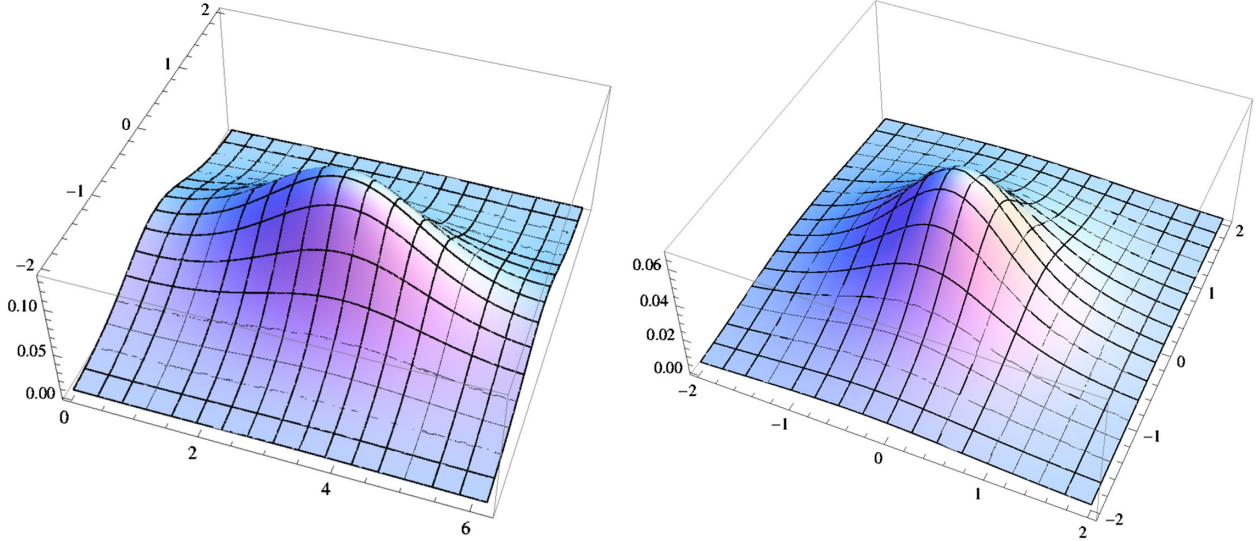


FIG. 4. Stationary solution of the Fokker-Planck equation of  $S = \beta \cos(x)$  for  $\beta = 0.25 + i0.5$ . Left:  $\rho(x, y)$  for  $0 \leq x \leq 2\pi$ . This function is periodic in  $x$  and  $\rho(x, y) = \rho(-x, -y)$ . Right:  $\sigma(X, Y)$ . In the numerical solution the matching was set at  $R_c = 2$ . For  $x \equiv \varphi$ , 64 Fourier modes were used and 64 points in the  $R$  and  $y$  grids. Numerical derivatives in  $R$  and  $y$  were obtained using 5 points.

Numerically, we obtain ( $\beta = 0.25 + i0.5$ )

$$\begin{aligned} \Delta P_1 - \frac{\beta}{2} \Delta P_2 &= -0.103539 + i0.207078, \\ -2\pi\beta^* \sigma(0) &= -0.103545 + i0.207089. \end{aligned} \quad (6.9)$$

The existence of a bias for complex  $\beta$  is consistent with similar findings in the recent work [37] which studies the analytically solvable two-dimensional Yang-Mills theory with a complex coupling constant.

### B. Other U(1) actions

One can consider more general actions of the form

$$S(x) = \sum_{k=n'}^n \beta_k e^{ikx} + imx, \quad n' \leq n. \quad (6.10)$$

The case  $n = n' = 0$  is of no interest (and it is not normalizable unless  $m = 0$ ) so either  $n > 0$  or  $n' < 0$  or both. Let us assume  $n > 0$  for definiteness. In this case, the analytically extended action  $S(z)$  will be dominated by the mode  $k = n$  for large negative  $y$ ; i.e., as regards to its behavior at  $y = -\infty$ , this action is equivalent to  $\beta_n e^{inz}$ . This is a periodic action with period  $2\pi/n$ , and in each period it is equivalent to the action  $\beta_n e^{iz}$  with  $z \in [0, 2\pi]$ , which brings us to Eq. (6.1) already studied. Therefore, barring accidental cancellations, one should expect that anomalies are generated at  $y = -\infty$  yielding a bias in the expectation values.

For a different generalization, one can consider a lattice with variables at sites or links and contributions of the type  $\beta \cos(\phi)$  to the action, with a chemical potential or other

mechanism making the variables to go to the complex plane. One can expect that the use of the complex Langevin algorithm will introduce a bias in the expectation value of the observables. The reason is that once the ensemble has reached the equilibrium, one can always keep updating the configurations without changing that equilibrium. This is true if one chooses to update just a single variable, and this leads us to the one-dimensional case we have been studying. In this view, a bias in the conditional distribution of a single variable implies a bias in the full distribution. On the other hand, updating just one variable is not the prescription of the standard complex Langevin algorithm, so this argument is not conclusive.

### VII. ANALYSIS OF A NONPERIODIC ACTION

We have already noted in the Introduction that a harmless looking action such as  $S = x^4/8 + 2ix$  cannot be reproduced by complex Langevin algorithm. The reason is that  $\langle e^{-ix} \rangle = -4.98$ , yet at equilibrium all Langevin walkers are below the real axis, so  $|\langle e^{-ix} \rangle_{\text{CL}}| \leq 1$ .

In this section we want to study the presence of anomalies in a nonperiodic system. Specifically, we consider the following one-dimensional action:

$$S(x) = \beta \frac{x^4}{4}, \quad \text{Re}\beta > 0. \quad (7.1)$$

Clearly, the symmetry  $S(x) = S(-x)$  will be shared by the complex Langevin equilibrium solution on the complex plane,

$$\rho(z) = \rho(-z), \quad z \in \mathbb{C}. \quad (7.2)$$

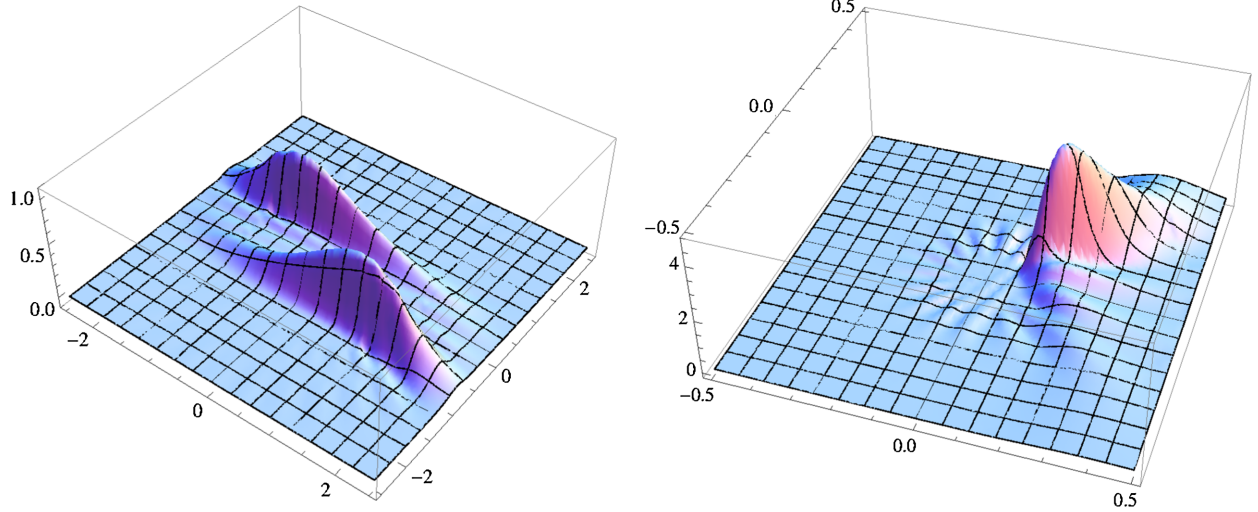


FIG. 5. The functions  $\rho(x, y)$  (left) and  $\sigma(X, Y)$  (right) for  $S = \beta x^4/4$  with  $\beta = 0.1 + i0.25$  and  $\lambda = 0$ . The matching is taken at  $r_c = 1.414$ . A 64 point mesh is used for the interval  $0 < r < r_c$  and 128 for  $0 < R < R_c$ . Thirty-two Fourier modes are used for  $\arg Z$  (corresponding to 64 modes for  $\arg z$ ). Numerically we find  $\sigma(0) = 0.011$  for this action.

The fixed point of the deterministic flow is at  $z = 0$ . It is attractive in one direction (the real axis rotated by  $\beta^{1/2}$ ) and repulsive in the orthogonal one.<sup>7</sup>

For convenience, we will allow an extra isotropic diffusion term in the complex Langevin process:

$$-\partial_t \rho = -\partial_x^2 \rho + \nabla \cdot (v\rho) - \lambda \nabla^2 \rho, \quad \lambda \geq 0. \quad (7.3)$$

As noted before, this is formally correct and the algorithm with nonvanishing  $\lambda$  has as much mathematical justification as the standard treatment. However the extra diffusion tends to spread the equilibrium distribution, thereby increasing the variance in the Monte Carlo calculation of the observables. Also, a possible anomaly is enhanced as regions away from the real axis become more populated. Mathematically, the equilibrium solution is better behaved for positive  $\lambda$ , in particular, we expect  $\rho(z)$  to be real analytic for all finite  $z$ .

For the action in Eq. (7.1), the Fokker-Planck equation, with  $\lambda$ , becomes

$$\begin{aligned} -\partial_t \rho = & -\beta \partial(z^3 \rho) - \beta^* \partial^*(z^{*3} \rho) - \partial^2 \rho - \partial^{*2} \rho \\ & - 2(1 + 2\lambda) \partial \partial^* \rho. \end{aligned} \quad (7.4)$$

Because the anomaly is related to the large  $y$  region, we will introduce a new set of coordinates  $(X, Y)$  centered at  $z = \infty$ . Specifically,

<sup>7</sup>Stationary points ( $S'_0 = 0$ ) which are nondegenerated ( $S''_0 \neq 0$ ), are either attractive [ $\text{Re}(S''_0) > 0$ ], repulsive [ $\text{Re}(S''_0) < 0$ ], or neutral [ $\text{Re}(S''_0) = 0$ ]; however,  $z = 0$  is a degenerated fixed point in our case.

$$Z = X + iY = \frac{1}{z^2}, \quad z = x + iy. \quad (7.5)$$

Let us denote by  $\sigma(X, Y)$  the density in the new coordinates,

$$\rho(z) = 4R^3 \sigma(Z), \quad R = |Z|. \quad (7.6)$$

Note that the  $Z$  plane only covers a half-plane of  $z$ . This is sufficient due to the symmetry  $z \rightarrow -z$  of  $\rho(z)$ . Of course,  $\sigma$  is normalized on the Riemann surface, so it has normalization  $1/2$  on the  $Z$  plane.

The new coordinate has been chosen so that the new deterministic flow has a finite velocity near  $Z = 0$ . Indeed, the Fokker-Planck equation in coordinates  $(X, Y)$  takes the form

$$\begin{aligned} -\partial_t \sigma = & \partial((2\beta + 6Z^2)\sigma) + \partial^*((2\beta^* + 6Z^{*2})\sigma) \\ & - 4\partial^2(Z^3 \sigma) - 4\partial^{*2}(Z^{*3} \sigma) - 8(1 + 2\lambda) \partial \partial^*(R^3 \sigma), \end{aligned} \quad (7.7)$$

and the velocity at  $Z = 0$  is  $2\beta$ .

Using the two sets of coordinates,  $z$  and  $Z$ , we have obtained numerical solutions for various values of  $\beta$  and  $\lambda$ . Similarly to the treatment in Sec. VI, the original coordinates  $(x, y)$  are used on a disk  $r = |z| \leq r_c$  and the new coordinates  $(X, Y)$  are used on  $R = |Z| \leq R_c$  with  $R_c = 1/r_c^2$ . The two solutions are matched at the boundary, imposing the condition of zero net flux there. This condition fixes the regularity condition at  $Z = 0$ . Grids are used for  $r$  and  $R$  and a finite number of Fourier modes are used for the angular variable. Numerical results for  $\rho(z)$  and  $\sigma(Z)$  with  $\beta = 0.1 + i0.5$  are displayed in Fig. 5 for  $\lambda = 0$  and Fig. 6 for  $\lambda = 0.5$ . As it would be expected,  $\rho$  is

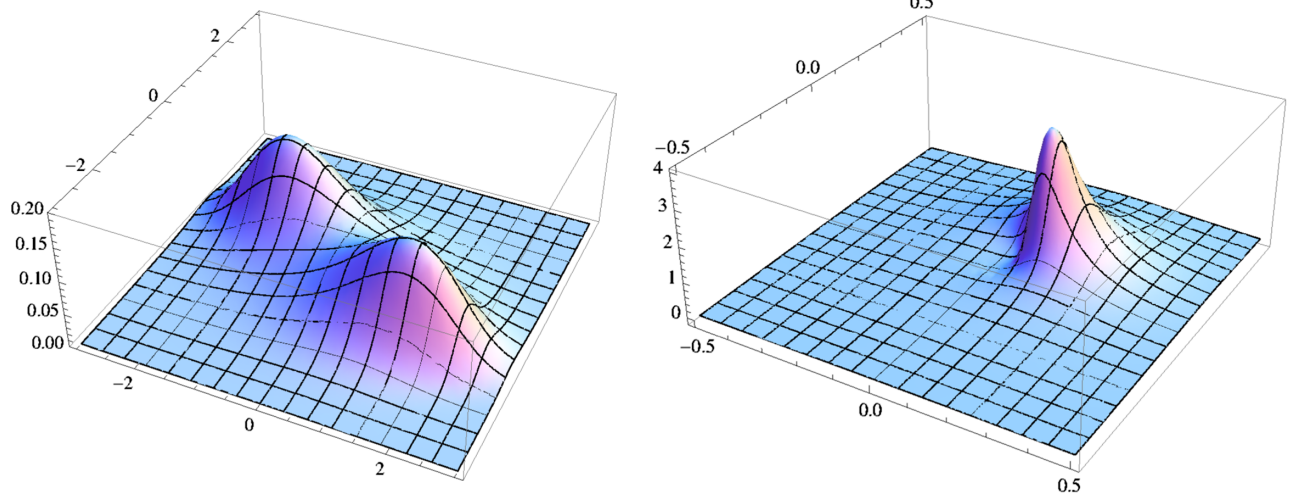


FIG. 6. Same as Fig. 5 for  $\lambda = 0.5$ . Numerically  $\sigma(0) = 0.292$ .

smoother and wider for  $\lambda = 0.5$  and also  $\sigma$  is larger near to  $Z = 0$ .

Numerically we find an anomaly in the expectation values. The effect is more visible for nonvanishing  $\lambda$  and this is the case we study in what follows. In order to elucidate the presence or not of an anomaly in the projected Fokker-Planck equation Eq. (3.17), we will analyze the behavior of  $\sigma(Z)$  in the region  $Z = 0$ , equivalent to large  $z$ . From inspection of the Fokker-Planck equation for  $\sigma$ , it follows that the diffusion does not play a dominant role near  $R = 0$ . In that region, the equilibrium equation can be simplified to

$$0 \approx \beta \partial \sigma + \beta^* \partial^* \sigma = \beta_R \partial_X \sigma + \beta_I \partial_Y \sigma, \quad \beta = \beta_R + i\beta_I. \quad (7.8)$$

Defining rotated variables

$$u = \frac{X}{\beta_R} - \frac{Y}{\beta_I}, \quad u' = \frac{X}{\beta_I} + \frac{Y}{\beta_R}, \quad (7.9)$$

Eq. (7.8) expresses that  $\sigma$  depends only on  $u$  and not on  $u'$ . We have verified this scaling in our numerical solution. In Fig. 7 we plot the values of  $\sigma(X, Y)$  against  $u$  in the region  $|y| \geq 3$  for the same action and  $\lambda$  as in Fig. 6. The result shows scaling, in the sense that  $u$  alone determines the value of  $\sigma$ .

Fig. 7 not only shows scaling in  $u$  in the large  $y$  limit, but it also suggests that  $\sigma(u)$  is actually rather flat. This can be understood as a consequence of the diffusion: the flux is constant along the flux lines and the diffusion (which is active not too close to  $Z = 0$ ) tends to equate the flux on the different lines, making the flux to be nearly constant everywhere. Near the origin, a constant flux implies a constant density  $\sigma$ , since there the velocity is almost constant. This observation suggests a simple model for

the behavior of  $\rho(x, y)$  in the region of large  $|y|$ , namely [using Eq. (7.6)]

$$\sigma \asymp \sigma(0), \quad \rho \asymp \rho_s(z) \equiv \frac{4\sigma(0)}{|z|^6} (|y| \rightarrow \infty). \quad (7.10)$$

The numerical validity of such asymptotic dependence is verified in Fig. 8. Figure 8(a) represents the ratio  $\rho/\rho_s$  on the  $(x, y)$  plane. This ratio is close to unity outside a bounded region around the origin  $z = 0$ . Figure 8(b) shows the marginal density  $N(y) = \int dx \rho(x, y)$  compared to that corresponding to  $\rho_s$ ,  $N_s(y) = 3\pi\sigma(0)/(2y^5)$ .

The combination of mathematical arguments and numerical evidence on the validity of the asymptotic form in Eq. (7.10) suggests that  $\rho_s(z)$  contains the relevant

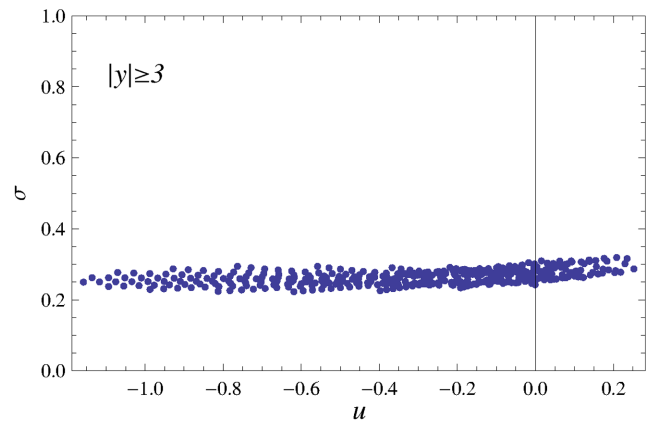


FIG. 7. For  $\beta = 0.1 + i0.25$  and  $\lambda = 0.5$ , values of the density  $\sigma(Z)$  plotted against the scaling variable  $u = X/\beta_R - Y/\beta_I$ . The 444 values shown correspond to a subset of the points used in the numerical solution of the differential equation (except that the 32 Fourier modes have been traded for 32 angular directions) defined by the condition  $|y| \geq 3$ . For these parameters  $\sigma(0) = 0.292$ .

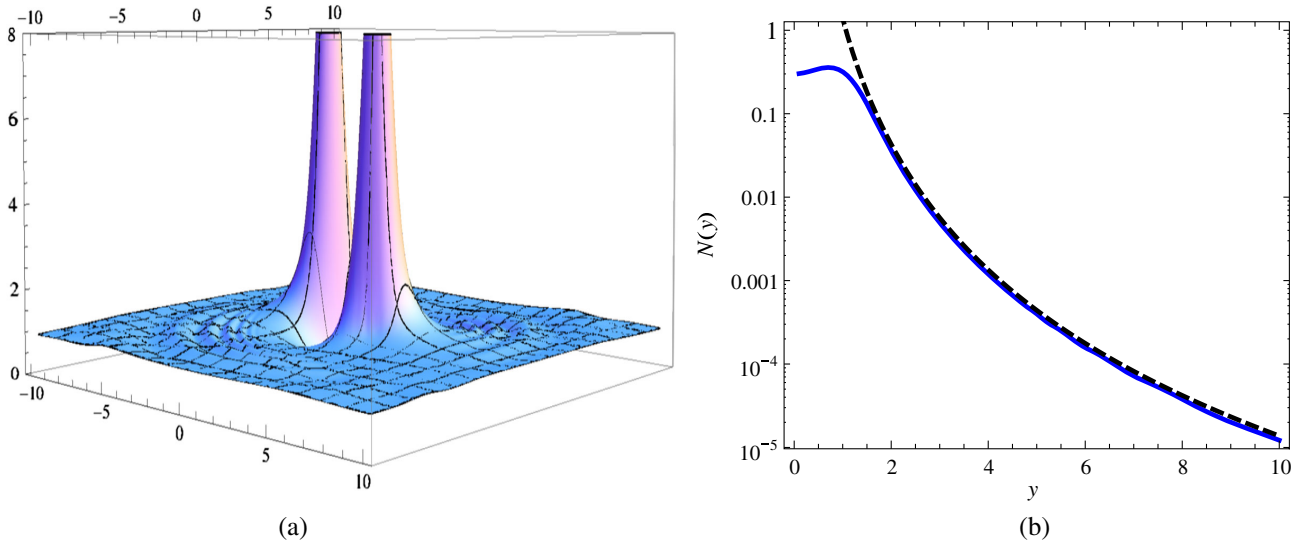


FIG. 8. For the solution of Fig. 6: (a) Ratio  $\rho/\rho_s = \sigma/\sigma(0)$  on the  $z$  plane.  $\rho$  is close to  $\rho_s$  in the asymptotic region. (b) Marginal probabilities  $N(y)$  of  $\rho$  (solid line, blue) and  $\rho_s$  (dashed line, black). They only differ in the region  $|y| < 2$ .

information regarding the existence of an anomaly in the projected Fokker-Planck equation. [Note however that we would really need to estimate  $\rho(x - iy, y)$  rather than  $\rho(x, y)$ .] In the presence of the new diffusion parameter  $\lambda$ , the anomaly (3.20) picks up an additional term and it is changed to

$$\begin{aligned} \mathcal{A}(x) &= -(v_y \rho + 2i\lambda \partial_z \rho)(x - iy, y)|_{y=-\infty}^{y=+\infty} \\ &\equiv \mathcal{A}(x)_+ - \mathcal{A}(x)_-. \end{aligned} \quad (7.11)$$

The new term with  $\lambda$  is more convergent than the standard one and so it is irrelevant to the anomaly. Nevertheless, the parameter  $\lambda$  has an indirect effect on the anomaly through its influence on  $\rho(z)$ . A direct calculation assuming that  $\rho_s$  saturates the anomaly gives

$$\mathcal{A}(x)_\pm = \frac{2i\beta^* \sigma(0)}{x^3}. \quad (7.12)$$

As expected the term with  $\lambda$  has a vanishing contribution in the  $|y| \rightarrow \infty$  limit.

As it stands  $\mathcal{A}(x)_+ = \mathcal{A}(x)_-$ , and the anomaly would cancel. In fact,  $P(x)$  is an even function, and  $\mathcal{A}(x)$  must also be even since parity is not broken by the Fokker-Planck equation. Hence, the  $\mathcal{A}(x)_\pm$  just found, which are odd functions, could never have a net contribution to the anomaly. However, the result is singular at  $x = 0$  and a local distribution of the same dimension,  $\delta''(x)$ , can be present upon regularization. Such a local distribution is an even function and would contribute to the anomaly. In order to have a regularized result we turn to the computation in momentum space. The anomaly in Eq. (7.11) takes the form

$$\tilde{\mathcal{A}}(k)_\pm = -e^{ky} (\tilde{v}_y * \tilde{\rho}_s + \lambda(\partial_y - k)\tilde{\rho}_s)|_{y=\pm\infty}. \quad (7.13)$$

Use of the relations  $\tilde{z}^* = i(\partial_k + y)$ ,  $\tilde{z}^{**} = i(\partial_k - y)$  in  $v_y = -(\beta z^3 - \beta^* z^{*3})/2i$  and

$$\tilde{\rho}_s(k, y) = 4\pi\sigma(0)(k^2 y^2 + 3|ky| + 3) \frac{e^{-|ky|}}{8|y|^5} \quad (7.14)$$

yields well-defined distributions in momentum space, namely,

$$\tilde{\mathcal{A}}(k)_\pm = \mp 2\pi\beta^* \sigma(0) k^2 \theta(\pm k), \quad (7.15)$$

which correspond to

$$\mathcal{A}(x)_\pm = 2i\beta^* \sigma(0) P \frac{1}{x^3} \pm \pi\beta^* \sigma(0) \delta''(x). \quad (7.16)$$

So finally, the assumption that  $\rho_s$  saturates the anomaly yields

$$\mathcal{A}(x) = 2\pi\beta^* \sigma(0) \delta''(x). \quad (7.17)$$

When this expression is introduced in the anomalous projected Fokker-Planck equation at equilibrium,

$$0 = \partial_x(vP - \partial_x P) - a\delta''(x), \quad a \equiv 2\pi\beta^* \sigma(0), \quad (7.18)$$

the normalized biased solution is obtained as

$$P(x) = (1 + a)P_0(x) - a\delta(x) \quad (7.19)$$

where  $P_0(x)$  is the normalized unbiased solution  $P_0 \propto e^{-\beta x^4/4}$ .



For a generic observable  $\mathcal{O}(x)$ , the anomalous expectation value becomes

$$\langle \mathcal{O} \rangle = (1 + a)\langle \mathcal{O} \rangle_0 - a\mathcal{O}(0), \quad (7.20)$$

where  $\langle \mathcal{O} \rangle_0$  is the unbiased result. In particular<sup>8</sup>

$$\langle x^n \rangle = (1 + a)\langle x^n \rangle_0, \quad n > 0. \quad (7.21)$$

This relation can be tested numerically. For  $\beta = 0.1 + i0.25$  and  $\lambda = 0.5$ ,  $a = 0.184 - 0.459i$ , and we obtain

$$\begin{aligned} \langle x^2 \rangle_0 &= 1.079 - 0.730i, & \langle x^4 \rangle_0 &= 1.379 - 3.448i, \\ \langle x^2 \rangle &= 0.946 - 1.238i, & \langle x^4 \rangle &= 0.107 - 4.664i, \\ (1 + a)\langle x^2 \rangle_0 &= 0.942 - 1.359i, \\ (1 + a)\langle x^4 \rangle_0 &= 0.050 - 4.714i. \end{aligned} \quad (7.22)$$

These results show that there is indeed a bias in the complex Langevin solution. Furthermore, the anomaly estimated from Eq. (7.17) gives a fair description of the bias in  $\langle x^2 \rangle$  and  $\langle x^4 \rangle$ . For higher powers the numerical errors accumulate and it is harder to draw definite conclusions. Also, in the most interesting case of  $\lambda = 0$ ,  $\sigma(0)$  is too small and any possible bias competes with the numerical error of the calculation.

It is possible that asymptotic subleading corrections to  $\rho_s$  could give a contribution to the anomaly. An easy calculation generalizes the result in Eq. (7.17). Specifically, a subleading term of the type

$$\frac{c_{n,m}}{|z|^6} \frac{1}{z^n z^{*m}} \quad (7.23)$$

in  $\rho$  would yield a contribution to  $\mathcal{A}(x)$  equal to

$$c_{n,m} \pi \beta^* \frac{(-1)^n}{(n+2)!} \delta_{m,0} \delta^{(n+2)}(x). \quad (7.24)$$

Such terms would modify the expectation values of higher powers of  $x$ .

Note that we have not directly applied the analytic projection operator  $K$  to  $\rho_s(z)$  to obtain an estimate of  $P(x)$ . From dimensional considerations, the projection of  $\rho_s(z)$  would yield a  $\delta^{(4)}(x)$  term. However, when this is analyzed in momentum space, it can be seen that the  $k^4$  term comes from the small  $y$  region, where the estimate  $\rho_s(z)$  is not reliable. If the small  $y$  region is removed, one obtains instead  $k^2$ , i.e., a  $\delta''(x)$  estimate for  $P(x)$ . The problem with this procedure is that it is not clear which part of the estimate is anomalous and which part is just a regular contribution from  $P_0(x) = e^{-S(x)}$ .

## VIII. SUMMARY AND CONCLUSIONS

As noted in the Introduction, very general complex probability distributions admit a representation on the complexified manifold. The goal of the complex Langevin method is to construct one such valid representation for  $e^{-S(x)}$ . While the method is certainly handy and elegant, in the Introduction it is shown that perfectly valid complex actions cannot be reproduced with this approach, just from an analysis of the support of  $\rho_{\text{CL}}(z)$  on the complexified manifold. Also it is shown that barring the cases of quadratic or real actions, the only known exact solution of a stationary Fokker-Planck solution [see Eqs. (3.1) and (3.2)] gives completely incorrect results, even for the two Fourier modes for which the integrals are absolutely convergent.

It was already known [7] that even if the projected Fokker-Planck equation is the naive one, spurious solutions of it can be selected by the algorithm. This is briefly reviewed in Sec. II. However, in practice such spurious solutions have to be enforced by using a suitable kernel or by choosing a complex probability with zeros or poles on the complex plane. A more pressing problem is discussed in Sec. III, namely, the emergence of an anomaly in the projected Fokker-Planck equation [see Eqs. (3.17) and (3.20)]. The anomaly  $\mathcal{A}(x)$  is a surface term which would be absent if the stationary density  $\rho(z)$  were sufficiently convergent far from the real manifold. Similar boundary terms have been described in the analysis of [51]. Here we provide a precise mathematical form to the anomaly which allows us to derive explicit anomalous relations between the behavior at infinity and the bias induced on the observables [see e.g., Eqs. (4.19), (6.8), or (7.21)].

In Sec. IV we analyze the one-dimensional periodic action  $\beta \cos(x) + imx$  (with real  $\beta$  and integer  $m$ ). This action is of interest because in a Monte Carlo simulation using the complex Langevin, correct expectation values are obtained for  $\cos(x)$  and  $\sin(x)$ . Also, the flow on the complex plane looks healthy and with suitable located fixed points [see Fig. 1, (right panel)], yet this is not guarantee of a correct behavior. As noted, the flow would be qualitatively similar when  $m$  is not an integer, and in that case the stochastic process would produce some necessarily periodic distribution which certainly would not be a representation of  $e^{-\beta \cos(x) - imx}$ , which is not a periodic function. Also, the anomaly depends on how often the Langevin walkers visit the remote regions far from the real manifold and this is not obvious from the topology of the flow. As it turns out, we are able to show that the anomaly does not affect the expectation values of Fourier modes with  $k = -1, 0, 1, 2, 3, \dots$  (for positive  $m$ ), and hence the complex Langevin method provides a stationary solution which correctly reproduces all those modes. However, an anomaly is present and all the  $k < -1$  modes are biased. This warns us that conclusions based solely on numerical experiments could be misleading.

<sup>8</sup> $\langle x^n \rangle_0 = (4/\beta)^{n/4} \Gamma(\frac{n+1}{4}) / \Gamma(\frac{1}{4})$  for even nonnegative  $n$ .

That an anomaly is necessarily present for the action  $\beta \cos(x) + imx$  is proven in detail in Sec. V. For positive  $m$ , the support of  $\rho(z)$  (the stationary solution of the complex Langevin process) lies entirely on the lower half plane. Our approach is to make a change of variables  $(x, y)$  to  $(X, Y)$  which effectively compactifies the large negative  $y$  region to a point; this is the origin in the new variables. We show that this point is perfectly regular for the stochastic process in the new variables [see Eq. (5.7) and Fig. 2], and in particular the density  $\sigma(X, Y)$  [related to  $\rho(x, y)$  by the Jacobian of the change of variables] is strictly nonzero at  $(X, Y) = 0$ . This suffices to show that there is an anomaly in the projected Fokker-Planck equation for this action [see Eq. (5.5)]. Further, we numerically solve the differential equation using a finite number of Fourier modes for the periodic variable  $x$  and a mesh for  $R$  (related to  $y$ ). This allows us to verify numerically all the relations previously derived.

The study of anomalies in more general periodic actions is addressed in Sec. VI. It is argued that the anomaly does not vanish in the general case. We analyze in some detail the actions of the form  $\beta \cos(x)$  for complex  $\beta$ . Once again, we use compactifying coordinates  $(X, Y)$  and show that the anomaly is controlled by the behavior of  $\sigma(X, Y)$  near  $X = Y = 0$  [see Eq. (6.6)]. For these actions the support of the stationary solution of the complex Langevin process is no longer restricted to a half-plane [although parity is preserved by  $\rho(z)$ ]. So we use simultaneously the original coordinates  $(x, y)$  and the new coordinates  $(X, Y)$  in two juxtaposed patches, in order to solve numerically the Fokker-Planck equation. The two partial solutions are matched by requiring that there is no net flux through the boundary of the patches. The numerical solution allows us to establish the unequivocal presence of an anomaly, and moreover, the corresponding predicted bias is correctly reproduced, at a numerical level [see Eq. (6.9)].

Finally, in Sec. VII, a nonperiodic action is analyzed, namely,  $S(x) = -\beta x^4/4$ , for  $\text{Re}\beta > 0$ . In this case, in order to compactify and regularize the problem at infinity, the change of variables  $Z = 1/z^2$  is applied. These coordinates cover half of the  $z$  plane but this is sufficient since  $\rho(z)$  is an even function. In this way, the Fokker-Planck equation is solved numerically in two patches (one including  $z = 0$ , the other  $Z = 0$ ) and the solutions are matched at the common boundary. Once again the behavior of  $\sigma(Z)$  near  $Z = 0$  is expected to determine the presence of an anomaly in the projected equation; however, the value found for  $\sigma(0)$  is numerically small, and this prevents us from establishing, in an unambiguous way, whether an anomaly is present or not. The same situation takes place in the expectation values: any possible bias competes with the numerical error in the calculation. In order to obtain a clearer case, an extra diffusion is added in the complex Langevin process controlled by a positive parameter  $\lambda$  [see Eq. (7.3)].

Such a term has been considered before in similar studies [32,51]. The extra diffusion, although formally correct, has a negative effect on the complex Langevin process as a Monte Carlo method, yet simultaneously it greatly improves the mathematical behavior of the stationary solution, regarding its analyticity. This is advantageous both for the numerical solution of the differential equation and for the analysis of asymptotic behaviors. As a consequence, for positive  $\lambda$ , we are able to unambiguously establish the existence of an anomaly and a bias in the expectation values [see Eq. (7.22)]. In fact, from the asymptotic analysis we obtain an analytical form for the anomaly [see Eq. (7.17)] which is fully confirmed by the numerical calculation.<sup>9</sup>

One could wonder if a better estimate would be obtained for the observables by chopping off somehow the anomaly-generating contributions in the  $\rho(z)$  produced by the complex Langevin. It is difficult to give a complete answer without entering into casuistic. Nevertheless, there are two cases which are quite clear. For the action  $S = x^4/8 + 2ix$  noted in the Introduction, after stabilization, the support of  $\rho(z)$  lies entirely below the real axis. Removing part of the support does not change this. So the expectation value of  $e^{-ix}$  would still be smaller than unity (in absolute value), while the correct result is roughly  $-5$ . Therefore, the error would be sizable anyway. Another clear case is that of  $S = i \cos(x)$ , with an exact solution for the Fokker-Planck equation  $\rho(x, y) \propto \text{sech}^2(y)$ . This (incorrectly) predicts the vanishing of all expectation values of  $e^{-ikx}$  (for  $k$  different from 0). If we remove all points in the complex plane with  $|y|$  larger than some cutoff, still the new  $\rho$  will be a function of  $y$  only, and it will produce the same incorrect expectation values.

Since the anomaly is due to too frequent visits of the Langevin walker to remote regions far from the real manifold, the use of new variables, in which  $y = \infty$  is a regular point, has played an important role our in the analysis of the anomaly. The choice of the new variables is such that for them  $y = \infty$  becomes a finite point, say  $Z = 0$ , but more importantly, the velocity of the drift in the new variables,  $V(Z)$ , is strictly finite in a neighborhood of  $Z = 0$ , that is, neither zero nor infinite. Also, the diffusion becomes negligible there, because a finite stochastic jump in  $z$  is a small jump in  $Z$ . This can be done systematically by choosing  $Z(z)$  such that (we discuss the one-dimensional case only, however, similar changes of variables can be carried out in higher dimensions)

$$\frac{dZ}{dz} = \frac{1}{v(z)}, \quad (8.1)$$

which yields ( $Z = X + iY$ )

<sup>9</sup>Actually, we first observed empirically the relation in Eq. (7.21), with  $a = c\beta^*\sigma(0)$  and  $c \approx 6$ .

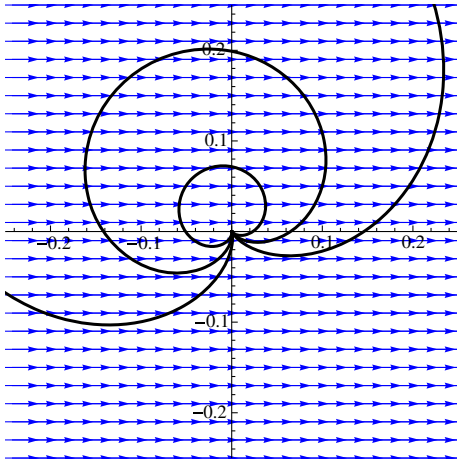


FIG. 9. Velocity field of  $S = \beta x^4/4$  in the variable  $Z = 1/(2\beta z^2)$ , for  $\beta = 0.1 + i0.25$ . The solid curves correspond to lines of  $x = \text{constant}$ , for  $x = 2, 3,$  and  $5$ . The diffusion randomly moves the Langevin walkers along these lines allowing them to visit a neighborhood of  $Z = 0$ . This suggests that  $\sigma(0)$ , or at least its limit from negative  $X$  if this function is not continuous at  $Z = 0$ , will not be exactly zero. [The peak of  $\sigma(X, Y)$  displayed in Fig. 5 falls at  $Z = 0.32 - i0.18$  here.]

$$-\partial_t \sigma = -\frac{1}{J} \partial_x^2 (J\sigma) + \partial_x \sigma, \quad (8.2)$$

with

$$\rho = J\sigma, \quad J = \frac{1}{|v(z)|^2}. \quad (8.3)$$

Up to corrections from the diffusion, this implies that the drift velocity  $V$  is constantly equal to 1, so the walkers move uniformly to the right. Essentially, these are the variables used in Eq. (7.5) for  $S = \beta x^4/4$ , and also in Eq. (5.1) for the periodic actions.<sup>10</sup>

When the Langevin walker follows an orbit of  $v(z)$  (let us obviate the diffusion at the moment) and this orbit visits a very remote region on the complex plane  $z$  before returning, in the  $Z$  plane this corresponds to a regular orbit passing near  $Z = 0$ . The fact that the velocity  $V$  is strictly finite there suggests that  $\sigma(0)$  will not be infinite (which would follow from  $V = 0$ ) nor zero (which would follow from  $V = \infty$ ). The point  $Z = 0$  (i.e.,  $z = \infty$ ) is a regular point and there is an orbit passing through it, taking a finite Langevin time to reach  $z = \infty$  and come back. The diffusion introduces irregularities but its effect is small in a neighborhood of  $Z = 0$ . Actually, the diffusion should help

<sup>10</sup>Actually, a velocity  $v = \sin(z)$  yields  $Z = \log(i \tan(z/2))$  [with  $\log(1) = 0$  and  $-\pi < \arg < \pi$ ], whereas the change in Eq. (5.1) is  $W = 2e^{ix+y}/(1 - e^{2y})$ ; however,  $Z = \log((W+1 - \sqrt{|W|^2+1})/(W-1 + \sqrt{|W|^2+1})) = -W^* + \frac{1}{12}(3W - W^*)W^{*2} + O(|W|^5)$  so the change of variables between the variables in Eq. (5.1) and Eq. (8.1) is regular and real analytic at  $Z = 0$ .

to flatten  $\sigma$  there: in general the walkers will have a chance to be moved to  $X < 0$  by diffusion (this is confirmed by studying the lines  $x = \text{constant}$  on the  $Z$  plane in the previous examples, see Fig. 2 and Fig. 9) and so inevitably the constant drift will move them to a neighborhood of  $Z = 0$ , implying that  $\sigma$  should be finite there. All this indicates that  $\sigma$  might be continuous and nonvanishing at  $Z = 0$  or at least have a finite limit from  $X < 0$ . The value of  $\sigma(0)$  might be exceedingly small in practice but nevertheless it would signal a bias in the algorithm.

Because we have seen in the various cases analyzed above that a nonnull  $\sigma(0)$  is tied to an anomaly, the arguments just presented tend to suggest that a nonnull anomaly, and so a bias in the estimates of the expectation values of the observables, would be the rule rather than the exception in the complex Langevin dynamics. An obvious objection is that the change of variable breaks down at the fixed points of  $v$ ; however, this is not a problem if the set of fixed points is bounded: in this case the change of variable is still well defined in a neighborhood of  $Z = 0$ , and a different coordinate can be used elsewhere. Alternatively, one can work on the Riemann surface; this is technically hard, but it does not invalidate the construction. A more substantial critique is that  $y = \infty$  needs not correspond to a finite  $Z$ . That the infinity of  $z$  can be brought to  $Z = 0$  follows from the explicit solution of Eq. (8.1)

$$Z = \int_{\infty}^z \frac{dz}{v}, \quad (8.4)$$

for points  $z$  lying beyond all the fixed points.<sup>11</sup> A problem arises if the integral is not convergent. This is the case for a quadratic action, since  $v \sim z$  for large  $z$ , and the integral diverges logarithmically. The integral converges provided  $v$  increases faster than  $|z|$  as  $|z| \rightarrow \infty$ . There is an intuitive explanation for this behavior. In fact,  $Z$  in Eq. (8.4) represents the time that the walker needs to reach infinity following an orbit of the field velocity. The integral converges if this time is finite. It seems to be a sensible criterion that when it takes only a finite time for the Langevin walker to arrive to infinity, the visits there will be frequent and  $\rho(z)$  will falloff much too slowly for the integration by parts to be justified. This introduces an anomaly and a bias in the expectation values. For a quadratic action the construction does not go through and an anomaly does not arise.

In order to investigate whether the anomaly could be obtained in closed form, let us momentarily assume that the regions  $y = \pm\infty$  are sufficiently well described by  $\sigma(Z) \approx \sigma_{\pm}(0)$ , where we allow two different values in the two regions. In this case the density can be approximated as

<sup>11</sup>Here we are assuming that  $y = \pm\infty$  have neighborhoods free from fixed points. These two patches need not overlap. A variable  $Z$  is defined in each patch.

$$\rho(z) \asymp \rho_{s,\pm}(z) \equiv \frac{\sigma_{\pm}(0)}{|v(z)|^2}, \quad y \rightarrow \pm\infty. \quad (8.5)$$

This formally yields for the anomaly, using Eq. (3.20),<sup>12</sup>

$$\begin{aligned} \mathcal{A}(x)_{\pm} &= - \left( \frac{v - v^* \sigma_{\pm}(0)}{2i v v^*} \right) (x - iy, y) \Big|_{y=\pm\infty} \\ &= - \frac{\sigma_{\pm}(0)}{2i} \left( \frac{1}{v(x + 2iy)^*} - \frac{1}{v(x)} \right) \Big|_{y=\pm\infty} \\ &= \frac{1}{2i} \frac{\sigma_{\pm}(0)}{v(x)}. \end{aligned} \quad (8.6)$$

This calculation would indicate that there is an anomaly if and only if  $\sigma_+(0) \neq \sigma_-(0)$ . [An exception would perhaps occur at the points where  $v(x) = 0$ , as seen in Sec. VII.] In particular, for even actions there would be no anomaly. However, we have shown that  $S = \beta \cos(x)$ , for instance, is anomalous. The paradoxical result is avoided by noting that the asymptotic relation  $\rho \asymp \rho_s$  refers to the limit  $y \rightarrow \infty$  with  $x$  fixed, while the anomaly requires to have a control on  $\rho$  in the limit  $\rho(x - iy, y)$  as  $y \rightarrow \infty$  with  $x$  fixed. This can be seen for the action  $S = i\beta_I \cos(x)$  for which  $\rho$  is known in closed form. In this case  $\sigma_{\pm}(0) = \beta_I^2/4\pi$ , so

$$\begin{aligned} \rho(x, y) &= \frac{1}{4\pi \cosh^2(y)} \asymp \frac{e^{-2|y|}}{\pi}, \\ \rho_s(x, y) &= \frac{\beta_I^2/4\pi}{\beta_I^2 |\sin(x + iy)|^2} \asymp \frac{e^{-2|y|}}{\pi}, \end{aligned} \quad (8.7)$$

and  $\rho_s$  correctly accounts for the behavior of  $\rho$  for large  $y$ . On the other hand, with fixed  $x$  and  $y \rightarrow \pm\infty$ ,

$$\begin{aligned} \rho(x - iy, y) &\asymp \frac{e^{-2|y|}}{\pi}, \\ \rho_s(x - iy, y) &\asymp \mp \frac{e^{\mp ix} e^{-2|y|}}{2i \sin(x) \pi}. \end{aligned} \quad (8.8)$$

The incorrect extra factor in  $\rho_s(x - iy, y)$ , as compared to  $\rho(x - iy, y)$ , produces the incorrect expression in Eq. (8.6) instead of Eq. (3.21).

The previous discussion indicates that a reasoning that correctly estimates  $\rho(x, y)$  in the  $y = \pm\infty$  regions does not necessarily suffice for describing the behavior of  $\rho(x - iy, y)$ , as required in the anomaly expressions. Nevertheless, it remains true that, in all cases analyzed, a nonvanishing value of  $\sigma(0)$  is tied to the presence of an anomaly and a bias in complex Langevin results, and we have argued that this will be the case quite generally. The numerical results do not allow us to clearly establish

whether  $\sigma(0)$  vanishes or not for  $S = \beta x^4/4$  with  $\lambda = 0$  (the interest of  $\lambda > 0$  is rather academic) but it seems clear that a positive value of  $\sigma(0)$  would yield an anomaly also in this case.

Another question is how these findings are modified by increasing the number of variables. Here we have studied one-dimensional problems, concluding that an anomaly is present quite generally, and this conclusion immediately extends to ultralocal actions, however, it is conceivable that, in general, the strength of the anomaly might depend on the dimension of the configuration manifold. In the instances in which the anomaly were decreasing to zero in the continuum or thermodynamic limits, the bias would eventually be screened by the standard Monte Carlo fluctuations and the method would be valid there. Also, a kernel modifies the algorithm while keeping its formal validity. It would be interesting to explore whether a suitable kernel could keep the walkers close to the real manifold thereby quenching or removing the anomaly. These points deserve further study.

We want to briefly comment on the relation between this work and the method of Lefschetz thimbles [25]. Like the complex Langevin, this technique to attack the sign problem also relies on the fact that the action is a holomorphic function. It amounts to trade the original real submanifold  $\mathbb{R}^n$  (embedded within the complex manifold of complex configurations  $\mathbb{C}^n$ ) by one or more cleverly chosen submanifolds of the same dimension, the Lefschetz thimbles, whose combination is homologous to the real submanifold, in the sense that holomorphic functions weighted with the Boltzmann factor of the action have the same integral in both treatments. (A smeared version of this technique is studied in [56]; another interesting extension can be found in [57].)

In the complex Langevin deterministic flow, nondegenerated fixed points are attractive or repulsive (or neutral) but not saddle points. Lefschetz thimbles are based on the gradient flow of  $\text{Re}(S)$  which shares the same fixed points, but now as saddle points. Passing through each fixed point there are two  $\text{Im}(S) = \text{constant}$  submanifolds, one for which the fixed point is a maximum of  $\text{Re}(S)$  and another for which is a minimum, the latter is the (stable) Lefschetz thimble associated to the fixed point (the other submanifold being the unstable thimble). This choice of integration manifold generalizes the stationary phase approximation. In practice, a subset of the (stable) thimbles have to be joined to form a manifold homologous to  $\mathbb{R}^n$  (namely, those whose fixed point have the unstable thimble intersecting  $\mathbb{R}^n$ ) [58].

Several studies have analyzed the relation between both techniques and how a wrong convergence of complex Langevin could be understood from the Lefschetz thimble point of view (see, e.g., [59]). Although this is not a fixed rule, the support of the complex Langevin distribution

<sup>12</sup>The result in Eq. (7.12) follows this scheme, albeit with a different normalization in  $\sigma$  since there  $Z = 1/z^2$  instead of  $1/(2\beta z^2)$ .

tends to follow the Lefschetz thimble and gives better results when there is a single dominant thimble. (A technique to enforce this feature as a way to improve complex Langevin is studied in [60].) Reference [61] finds that complex Langevin fails if multiple Lefschetz thimbles dominantly contribute with different complex phases. In fact, if there is just one dominant thimble this will usually correspond to the basin of a stable fixed point of the complex Langevin dynamics; however, if additional thimbles corresponding to *repulsive* points are relevant, such regions will not be visited by the Langevin walker and one can expect a bias in the estimates. For another argument related to the present work, the thimbles are boundaryless noncompact  $n$ -dimensional manifolds in  $\mathbb{C}^n$ . Keeping those having a contribution and with suitable orientation, their union forms a manifold homologous to  $\mathbb{R}^n$ . Typically when there is more than one (contributing) fixed point, the thimble stems from the fixed point towards infinity and there joins with the thimble of another fixed point.<sup>13</sup> Although the deterministic flow of complex Langevin and the gradient flow of  $\text{Re}(S)$  are different, they coincide asymptotically [59]. This means that when two relevant thimbles join at infinity they do so at a runaway trajectory of the Langevin walker. If the walker has to visit both thimbles for a proper sampling it necessarily must expend some time at infinity and this introduces an anomaly. This

<sup>13</sup>The union of thimbles is homologous to  $\mathbb{R}^n$  so they have to join somehow, but each thimble carries a different value of  $\text{Im}(S)$ ; the only solution is their joining at infinity.

would be a relation between the problems observed in complex Langevin when there is more than one dominant thimble and the presence of an anomaly in the projected Fokker-Planck equation. This heuristic argument implicitly assumes that a proper sampling can only be achieved when the support of the complex Langevin walker is close to the support of the relevant thimbles. A possible caveat though is that each thimble carries a different global phase and also a local phase through the Jacobian since the thimbles are not horizontal submanifolds in general. In other words, the thimbles do not define a proper representation with positive weight as defined in the Introduction, and this would account for the different supports in the two treatments. In this regard, it is interesting to point out that in [40] it is shown that any periodic action in any number of dimensions, can be represented using just two horizontal submanifolds, with positive weights on them, and the method has been extended to nonperiodic actions in [23] (albeit in the one-dimensional case). In this view, the study of the systematic construction of such two-branch representation seems worthwhile.

### ACKNOWLEDGMENTS

This work was supported by Spanish Ministerio de Economía y Competitividad and European FEDER funds (Grant No. FIS2014-59386-P), and by the Agencia de Innovación y Desarrollo de Andalucía (Grant No. FQM225). I thank an anonymous referee for providing the heuristic argument on runaway trajectories of Langevin walkers and Lefschetz thimbles.

- 
- [1] J. Glimm and A. M. Jaffe, *Quantum Physics: A Functional Integral Point Of View* (Springer, New York, 1987).
  - [2] P. Hasenfratz and F. Karsch, Chemical potential on the lattice, *Phys. Lett.* **125B**, 308 (1983).
  - [3] M. Troyer and U.J. Wiese, Computational Complexity and Fundamental Limitations to Fermionic Quantum Monte Carlo Simulations, *Phys. Rev. Lett.* **94**, 170201 (2005).
  - [4] G. Parisi, On complex probabilities, *Phys. Lett.* **131B**, 393 (1983).
  - [5] H. W. Hamber and H. c. Ren, Complex probabilities and the Langevin equation, *Phys. Lett.* **159B**, 330 (1985).
  - [6] G. Bhanot, A. Gocksch, and P. Rossi, On simulating complex actions, *Phys. Lett. B* **199**, 101 (1987).
  - [7] L. L. Salcedo, Spurious solutions of the complex Langevin equation, *Phys. Lett. B* **305**, 125 (1993).
  - [8] T. D. Kieu and C. J. Griffin, Monte Carlo simulations with indefinite and complex valued measures, *Phys. Rev. E* **49**, 3855 (1994).
  - [9] L. L. Salcedo, Representation of complex probabilities, *J. Math. Phys.* **38**, 1710 (1997).
  - [10] I. M. Barbour, S. E. Morrison, E. G. Klepfish, J. B. Kogut, and M. P. Lombardo, Results on finite density QCD, *Nucl. Phys. B, Proc. Suppl.* **60A**, 220 (1998).
  - [11] S. Chandrasekharan and U.J. Wiese, Meron Cluster Solution of a Fermion Sign Problem, *Phys. Rev. Lett.* **83**, 3116 (1999).
  - [12] Z. Fodor and S. D. Katz, A new method to study lattice QCD at finite temperature and chemical potential, *Phys. Lett. B* **534**, 87 (2002).
  - [13] N. Prokof'ev and B. Svistunov, Worm Algorithms for Classical Statistical Models, *Phys. Rev. Lett.* **87**, 160601 (2001).
  - [14] S. A. Baurle, Method of Gaussian Equivalent Representation: A New Technique for Reducing the Sign Problem of Functional Integral Methods, *Phys. Rev. Lett.* **89**, 080602 (2002).

- [15] A. G. Moreira, S. A. Baurle, and G. H. Fredrickson, Global Stationary Phase and the Sign Problem, *Phys. Rev. Lett.* **91**, 150201 (2003).
- [16] V. Azcoiti, G. Di Carlo, A. Galante, and V. Laliena, Finite density QCD: A new approach, *J. High Energy Phys.* **12** (2004) 010.
- [17] J. Berges and I.-O. Stamatescu, Simulating Nonequilibrium Quantum Fields with Stochastic Quantization Techniques, *Phys. Rev. Lett.* **95**, 202003 (2005).
- [18] G. Aarts, Can Stochastic Quantization Evade the Sign Problem? The Relativistic Bose Gas at Finite Chemical Potential, *Phys. Rev. Lett.* **102**, 131601 (2009).
- [19] D. Banerjee and S. Chandrasekharan, Finite size effects in the presence of a chemical potential: A study in the classical nonlinear  $O(2)$  sigma model, *Phys. Rev. D* **81**, 125007 (2010).
- [20] J. Bloch, Evading the Sign Problem in Random Matrix Simulations, *Phys. Rev. Lett.* **107**, 132002 (2011).
- [21] M. Cristoforetti, F. Di Renzo, A. Mukherjee, and L. Scorzato, Monte Carlo simulations on the Lefschetz thimble: Taming the sign problem, *Phys. Rev. D* **88**, 051501 (2013).
- [22] R. Rota, J. Casulleras, F. Mazzanti, and J. Boronat, Quantum Monte Carlo estimation of complex-time correlations for the study of the ground-state dynamic structure function, *J. Chem. Phys.* **142**, 114114 (2015).
- [23] L. L. Salcedo, Gibbs sampling of complex-valued distributions, *Phys. Rev. D* **94**, 074503 (2016).
- [24] J. S. Liu, *Monte Carlo Strategies in Scientific Computing* (Springer, New York, 2001).
- [25] M. Cristoforetti, F. Di Renzo, and L. Scorzato, New approach to the sign problem in quantum field theories: High density QCD on a Lefschetz thimble, *Phys. Rev. D* **86**, 074506 (2012).
- [26] H. Hufel and H. Rumpf, Stochastic quantization in Minkowski space, *Phys. Lett.* **148B**, 104 (1984).
- [27] J. Ambjorn, M. Flensburg, and C. Peterson, The complex Langevin equation and Monte Carlo simulations of actions with static charges, *Nucl. Phys.* **B275**, 375 (1986).
- [28] J. Berges, S. Borsanyi, D. Sexty, and I.-O. Stamatescu, Lattice simulations of real-time quantum fields, *Phys. Rev. D* **75**, 045007 (2007).
- [29] I. Barbour, N.E. Behlil, E. Dagotto, F. Karsch, A. Moreo, M. Stone, and H.W. Wyld, Problems with finite density simulations of lattice QCD, *Nucl. Phys.* **B275**, 296 (1986).
- [30] P.H. Damgaard and H. Hufel, Stochastic quantization, *Phys. Rep.* **152**, 227 (1987).
- [31] K. Fukushima and T. Hatsuda, The phase diagram of dense QCD, *Rep. Prog. Phys.* **74**, 014001 (2011).
- [32] G. Aarts, F.A. James, E. Seiler, and I.O. Stamatescu, Complex Langevin: Etiology and diagnostics of its main problem, *Eur. Phys. J. C* **71**, 1756 (2011).
- [33] C. Pehlevan and G. Guralnik, Complex Langevin equations and Schwinger-Dyson equations, *Nucl. Phys.* **B811**, 519 (2009).
- [34] J. Ambjorn, M. Flensburg, and C. Peterson, Langevin simulations of configurations with static charges, *Phys. Lett.* **159B**, 335 (1985).
- [35] J. Bloch, J. Mahr, and S. Schmalzbauer, Complex Langevin in low-dimensional QCD: The good and the not-so-good, *Proc. Sci.*, LATTICE2015 (2016) 158 [arXiv:1508.05252].
- [36] J. Ambjorn and S. K. Yang, Numerical problems in applying the Langevin equation to complex effective actions, *Phys. Lett.* **165B**, 140 (1985).
- [37] H. Makino, H. Suzuki, and D. Takeda, Complex Langevin method applied to the 2D  $SU(2)$  Yang-Mills theory, *Phys. Rev. D* **92**, 085020 (2015).
- [38] B. Soderberg, On the complex Langevin equation, *Nucl. Phys.* **B295**, 396 (1988).
- [39] D. Weingarten, Complex Probabilities on  $R^N$  as Real Probabilities on  $C^N$  and an Application to Path Integrals, *Phys. Rev. Lett.* **89**, 240201 (2002).
- [40] L. L. Salcedo, Existence of positive representations for complex weights, *J. Phys. A* **40**, 9399 (2007).
- [41] J. Wosiek, Beyond complex Langevin equations I: Two simple examples, arXiv:1511.09083.
- [42] J. Wosiek, Beyond complex Langevin equations II: A positive representation of Feynman path integrals directly in the Minkowski time, *J. High Energy Phys.* **04** (2016) 146.
- [43] K. Fujimura, K. Okano, L. Schulke, K. Yamagishi, and B. Zheng, On the segregation phenomenon in complex Langevin simulation, *Nucl. Phys.* **B424**, 675 (1994).
- [44] C. Adami and S. E. Koonin, Complex Langevin equation and the many fermion problem, *Phys. Rev. C* **63**, 034319 (2001).
- [45] H. Gausterer, Complex Langevin: A numerical method?, *Nucl. Phys.* **A642**, c239 (1998).
- [46] E. Gozzi, Langevin simulation in Minkowski space, *Phys. Lett.* **150B**, 119 (1985).
- [47] S. Lee, The convergence of complex Langevin simulations, *Nucl. Phys.* **B413**, 827 (1994).
- [48] H. Gausterer and J.R. Klauder, Complex Langevin Solution of the Schwinger Model, *Phys. Rev. Lett.* **56**, 306 (1986).
- [49] J.R. Klauder and W.P. Petersen, Spectrum of certain non-self-adjoint operators and solutions of Langevin equations with complex drift, *J. Stat. Phys.* **39**, 53 (1985).
- [50] R. W. Haymaker and J. Wosiek, Complex Langevin simulations of non-Abelian integrals, *Phys. Rev. D* **37**, 969 (1988).
- [51] G. Aarts, E. Seiler, and I. O. Stamatescu, Complex Langevin method: When can it be trusted?, *Phys. Rev. D* **81**, 054508 (2010).
- [52] K. Nagata, J. Nishimura, and S. Shimasaki, The argument for justification of the complex Langevin method and the condition for correct convergence, arXiv:1606.07627.
- [53] J. Nishimura and S. Shimasaki, New insights into the problem with a singular drift term in the complex Langevin method, *Phys. Rev. D* **92**, 011501 (2015).
- [54] H. Okamoto, K. Okano, L. Schulke and S. Tanaka, The role of a kernel in complex Langevin systems, *Nucl. Phys.* **B324**, 684 (1989).
- [55] F. Karsch and H. W. Wyld, Complex Langevin Simulation of the  $SU(3)$  Spin Model With Nonzero Chemical Potential, *Phys. Rev. Lett.* **55**, 2242 (1985).

- [56] K. Fukushima and Y. Tanizaki, Hamilton dynamics for Lefschetz-thimble integration akin to the complex Langevin method, *Prog. Theor. Exp. Phys.* (2015) 111A01.
- [57] A. Alexandru, G. Basar, P. F. Bedaque, G. W. Ridgway, and N. C. Warrington, Sign problem and Monte Carlo calculations beyond Lefschetz thimbles, *J. High Energy Phys.* 05 (2016) 053.
- [58] E. Witten, Analytic continuation of Chern-Simons theory, in *Chern-Simons Gauge Theory: 20 Years After*, edited by J. E. Andersen, H. U. Boden, A. Hahn, and B. Himpel, AMS/IP Stud. Adv. Math. Vol. 50 (American Mathematical Society, Providence, 2011), p. 347.
- [59] G. Aarts, L. Bongiovanni, E. Seiler, and D. Sexty, Some remarks on Lefschetz thimbles and complex Langevin dynamics, *J. High Energy Phys.* 10 (2014) 159.
- [60] S. Tsutsui and T. M. Doi, Improvement in complex Langevin dynamics from a view point of Lefschetz thimbles, *Phys. Rev. D* **94**, 074009 (2016).
- [61] T. Hayata, Y. Hidaka, and Y. Tanizaki, Complex saddle points and the sign problem in complex Langevin simulation, *Nucl. Phys.* **B911**, 94 (2016).